

E 201 994

AD-A280 947

①



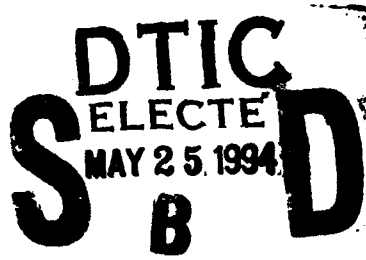
PL-TR-94-2036

SSS-TR-94-14399

**Seismic Identification Analyses of Cavity Decoupled Nuclear
and Chemical Explosions**

**John R. Murphy
Brian W. Barker**

**Maxwell Laboratories, Incorporated
S-CUBED Division
P.O. Box 1620
La Jolla, CA 92038-1620**



January 1994

838 94-15530

Scientific Report No. 2

Approved for public release; distribution unlimited

DTIC QUALITY INSPECTED 5

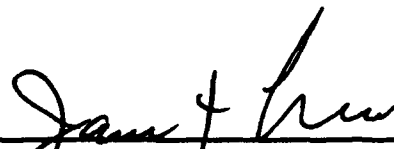


**PHILLIPS LABORATORY
Directorate of Geophysics
AIR FORCE MATERIEL COMMAND
HANSCOM AIR FORCE BASE, MA 01731-3010**

94 5 23 118

The views and conclusions contained in this document are those of the authors and should not be interpreted as representing the official policies, either express or implied, of the Air Force or the U.S. Government.

This technical report has been reviewed and is approved for publication.


JAMES F. LEWKOWICZ
Contract Manager
Earth Sciences Division


JAMES F. LEWKOWICZ, Director
Earth Sciences Division

This report has been reviewed by the ESC Public Affairs Office (PA) and is releasable to the National Technical Information Service (NTIS).

Qualified requestors may obtain additional copies from the Defense Technical Information Center. All others should apply to the National Technical Information Service.

If your address has changed, or if you wish to be removed from the mailing list, or if the addressee is no longer employed by your organization, please notify PL/TSI, 29 Randolph Road, Hanscom AFB, MA 01731-3010. This will assist us in maintaining a current mailing list.

Do not return copies of this report unless contractual obligations or notices on a specific document requires that it be returned.

REPORT DOCUMENTATION PAGE			Form Approved OMB No. 0704-0188	
<small>Public reporting burden for this collection of information is estimated to average 1 hour per response, including the time for reviewing instructions, searching existing data sources, gathering and maintaining the data needed, and completing and reviewing the collection of information. Send comments regarding this burden estimate or any other aspect of this collection of information, including suggestions for reducing this burden, to Washington Headquarters Services, Directorate for Information Operations and Reports, 1215 Jefferson Davis Highway, Suite 1204, Arlington, VA 22202-4302, and to the Office of Management and Budget, Paperwork Reduction Project (0704-0188), Washington, DC 20503.</small>				
1. AGENCY USE ONLY (Leave blank)		2. REPORT DATE January, 1994		3. REPORT TYPE AND DATES COVERED Scientific No. 2
4. TITLE AND SUBTITLE Seismic Identification Analyses of Cavity Decoupled Nuclear and Chemical Explosions			5. FUNDING NUMBERS Contract: F19628-91-C-0186 PE 61102F PR 2309 TA G2 WUBL	
6. AUTHOR(S) John R. Murphy and Brian W. Barker				
7. PERFORMING ORGANIZATION NAME(S) AND ADDRESS(ES) Maxwell Laboratories, Inc. S-CUBED Division P.O. Box 1620 La Jolla, CA 92038-1620			8. PERFORMING ORGANIZATION REPORT NUMBER SSS-TR-94-14399	
9. SPONSORING/MONITORING AGENCY NAME(S) AND ADDRESS(ES) Phillips Laboratory 29 Randolph Road Hanscom AFB, MA 01731-3010 Contract Manager: James F. Lewkowicz/GPEH			10. SPONSORING/MONITORING AGENCY REPORT NUMBER PL-TR-94-2036	
11. SUPPLEMENTARY NOTES				
12a. DISTRIBUTION/AVAILABILITY STATEMENT Approved for public release; distribution unlimited			12b. DISTRIBUTION CODE	
13. ABSTRACT (Maximum 200 words) <p>Successful seismic monitoring of any eventual Comprehensive Test Ban Treaty will require the development of a capability to identify signals from small cavity decoupled nuclear explosions from among the numerous signals to be expected from earthquakes, rockbursts and chemical explosion (CE) events of comparable magnitude. The investigations summarized in this report focus on preliminary studies which have been carried out in an attempt to distinguish between decoupled nuclear explosions and CE events through analyses of observed and simulated seismic data for these two source types in both the U.S. and former Soviet Union.</p> <p>Near-regional seismic data recorded from the U.S. nuclear cavity decoupling test STERLING and the nearby tamped CE test STERLING HE are compared in Section II in an attempt to identify diagnostic differences between these two source types. This is followed in Section III by an analysis in which short-period P wave data recorded at NORSAR from Soviet nuclear tests conducted in salt cavities</p> <p>(continued on reverse)</p>				
14. SUBJECT TERMS Seismic Explosion Nuclear STERLING Discrimination Cavity Decoupling Mine Blast Azgir			15. NUMBER OF PAGES 82	
			16. PRICE CODE	
17. SECURITY CLASSIFICATION OF REPORT UNCLASSIFIED	18. SECURITY CLASSIFICATION OF THIS PAGE UNCLASSIFIED	19. SECURITY CLASSIFICATION OF ABSTRACT UNCLASSIFIED	20. LIMITATION OF ABSTRACT UNLIMITED	

DECLASSIFY ON:

13. ABSTRACT (Continued)

at the Azgir site north of the Caspian Sea are systematically compared with corresponding data recorded at the same stations from presumed CE events of comparable size which have been located in the vicinity of the Azgir site. In Section IV, broadband seismic data recorded at near-regional Soviet stations from an Azgir nuclear cavity decoupling test are theoretically scaled to the 1 kt fully decoupled level and compared with data recorded at the nearby IRIS station KIV from well-documented CE events. The results of these preliminary comparison studies indicate that seismic discrimination between these two explosion source types is not trivial and suggest that a reliable discrimination strategy will have to be based on detailed analysis of data from multiple seismic phases.

Table of Contents

1.	Introduction	1
2.	Comparison of Broadband Near-Regional Seismic Signals Recorded from the STERLING and STERLING HE Explosions.....	3
3.	Comparison of P Wave Signals Recorded at NORSAR from CE and Nuclear Cavity Explosions in the North Caspian Basin	19
4.	Comparison of Broadband Near-Regional Seismic Recordings from Soviet CE and Cavity Decoupled Explosions in the Caspian Sea Region	43
5.	Summary and Conclusions	62
	5.1 Summary.....	62
	5.2 Conclusions	63
	References.....	66

Accession For	
NTIS GRA&I	<input checked="" type="checkbox"/>
DTIC TAB	<input type="checkbox"/>
Unannounced	<input type="checkbox"/>
Justification	
By _____	
Distribution/ _____	
Availability Codes	
Dist	Avail and/or Special
A-1	

List of Illustrations

		PAGE
1	Vertical component time histories at station 10S for STERLING (top) and STERLING HE (bottom). Arrows indicate approximate start of S-wave window.....	5
2	Vertical component time histories at station 20S for STERLING (top) and STERLING HE (bottom). Arrows indicate approximate start of S-wave window.....	6
3	Relative P-wave amplitude spectra at station 10S for STERLING (top) and STERLING HE (bottom).....	8
4	Relative P-wave amplitude spectra at station 20S for STERLING (top) and STERLING HE (bottom).....	9
5	Relative S-wave amplitude spectra from station 10S (top) and 20S (bottom) for STERLING and STERLING HE.....	11
6	Comparison of S/P amplitude ratios versus frequency for STERLING and STERLING HE determined from narrowband filter analysis of near-regional waveforms recorded at stations 10S (left) and 20S (right).....	13
7	Source locations of STERLING and STERLING HE with respect to the boundary of the Tatum salt dome at source depth.....	15
8	Comparison of initial charge geometries for STERLING, STERLING HE and the NTS chemical kiloton explosion. ...	16
9	Epicenters of earthquakes with $K > 11$ in the Caspian region developed from Russian earthquake catalogs for the period 1962 to 1979.....	20

10	Figure 10. Locations of events reported by NORSAR for the aseismic area bounded by 45°N and 52°N and by 42°E and 55°E during the time period from October, 1971 to October, 1981.....	22
11	Comparison of the distribution of times of occurrence of the seismic events from Ringdal's north Caspian list (top) with that for natural earthquakes from the Caucasus area to the south (bottom).	23
12	NORSAR locations of the selected Caspian events. Open circles denote nuclear cavity tests while asterisks denote presumed chemical explosions.....	26
13	NORSAR subarray element O2B0 recordings of selected Caspian seismic events.....	28
14	Filtered (0.8-6.0 Hz) NORSAR subarray element O2B0 recordings of selected Caspian events.....	29
15	NORSAR subarray O2B P wave signal (solid line) and noise (dashed line) spectra for Event #1.....	31
16	NORSAR subarray O2B P wave signal (solid line) and noise (dashed line) spectra for Event #4.....	32
17	NORSAR subarray O2B P wave signal (solid line) and noise (dashed line) spectra for Event #10.....	33
18	NORSAR O2B single element (left) and subarray-averaged (right) P wave spectra for Event #1.....	34
19	NORSAR O2B single element (left) and subarray-averaged (right) P wave spectra for Event #4.....	35
20	NORSAR O2B single element (left) and subarray-averaged (right) P wave spectra for Event #10.....	36
21	Comparison of NORSAR O2B subarray-averaged P wave spectra for Events #1-#3.	37

22	Comparison of NORSAR O2B subarray-averaged P wave spectra for Events #4-#8.	38
23	Comparison of NORSAR O2B subarray-averaged P wave spectra for Events #9-#12.....	39
24	Comparison of NORSAR O2B P wave spectral average for Events #1-#3 with corresponding averages for Events #4-#8 and Events #9-#12.....	41
25	Comparison of ratios of average spectra for the two HE groups of events computed with respect to the spectrum for cavity decoupled nuclear Event #9.....	42
26	Comparison of observed SALMON and scaled STERLING (SALMON synthetic) radial component seismograms for station 10S.	48
27	Comparison of observed SALMON free-field particle velocity recording at a range of 166 m with the cube-root scaled Azgir 4/22/66 free-field particle velocity recording at a scaled range (at 5.3 kt) of 142 m.....	49
28	Vertical component ground motions recorded from the 8 kt Azgir cavity decoupling test of 3/29/76.....	51
29	Comparison of approximate source scaling operators for partially (dashed) and fully (solid) decoupled 1 kt explosions, estimated relative to the partially decoupled 8 kt Azgir cavity explosion of 3/29/76.....	52
30	Theoretically scaled vertical component ground motions corresponding to a 1 kt fully decoupled explosion at the source location of the 8 kt Azgir decoupling test of 3/29/76.....	54
31	Estimated peak vertical displacements as a function of distance for a fully decoupled 1 kt cavity explosion at Azgir.	55

32	Map location of IRIS station KIV with respect to the Azgir test site. The expanded display at the right shows the locations of selected mines and broadband recording stations around KIV.....	57
33	Comparison of peak vertical displacement levels observed from three well-documented Caspian mine blasts (solid) with the corresponding displacement levels expected from a fully decoupled 1 kt nuclear explosion at Azgir (dashed). ...	58
34	Comparison of scaled Azgir 1 kt fully decoupled ground motion estimates with the ground motions recorded in the same near-regional distance range from CE blasts at the Tyrnyauz mine.....	60

1. Introduction

As a result of research conducted over the past 20 years, the capability now exists to unambiguously identify almost all seismic events having magnitudes characteristic of well-coupled, underground nuclear explosions with yields greater than a few kilotons (i.e. $m_b \gtrsim 4$, OTA (1988)). However, in the context of monitoring any eventual Comprehensive Test Ban Treaty (CTBT), consideration will have to be given to the capability for identifying the much smaller signals which might be expected to result from possible evasive testing involving cavity decoupling. That is, since the U.S. nuclear cavity decoupling experiment STERLING has established that it is possible to reduce the amplitude of the radiated seismic signal by a least a factor of 70 using this testing procedure, it follows that comprehensive monitoring of underground nuclear tests in the 1 to 10 kt range will necessarily involve identification analyses of small seismic events with magnitudes in the range $2 < m_b < 3$. Moreover, at such low magnitudes, naturally occurring earthquakes are supplemented by a large number of chemical explosions (CE) of similar size which are associated with the variety of quarrying, mining and construction projects which are continuously being carried out in most developed areas of the world. This constitutes a potentially serious monitoring problem in that there are no consistently reliable procedures available at the present time for distinguishing between seismic signals produced by cavity decoupled nuclear and chemical explosions. Thus, even assuming the existence of the very extensive monitoring networks needed to detect such small events, questions remain concerning our capability to correctly identify the signals from small decoupled explosions among the numerous signals expected from earthquakes and CE events of comparable size. The objective of the research program described in this report is to improve the capability to distinguish between small cavity decoupled nuclear explosions and CE events through analyses of simulated and observed seismic data representative of the two source types.

This report presents a summary of the preliminary investigations which have been conducted during the first year of this project. In Section 2, near-regional seismic data recorded from the U.S. nuclear cavity decoupling test STERLING and the nearby, tamped CE test, denoted STERLING HE, are analyzed and compared in an attempt to identify any diagnostic differences between these two source types. This is followed in Section 3 by an analysis in which seismic data recorded at NORSAR from Soviet nuclear tests conducted in salt cavities at the Azgir site north of the Caspian Sea are compared with corresponding data recorded at the same stations from events of about the same size which appear to be CE events conducted in the vicinity of the Azgir site. In Section 4, broadband seismic data recorded at near-regional Soviet stations from an Azgir cavity decoupling test are theoretically scaled and compared with data recorded at similar distances at the nearby IRIS station KIV from well-documented CE events. The report concludes with Section 5 which contains a summary and statement of preliminary conclusions regarding the identification of seismic signals recorded from cavity decoupled nuclear and chemical explosions.

2. Comparison of Broadband Near-Regional Seismic Signals Recorded from the STERLING and STERLING HE Explosions

The SALMON, STERLING and STERLING HE explosions were conducted in the Tatum salt dome near Hattiesburg, Mississippi between 1964 and 1966 with the objective of evaluating the effectiveness of cavity decoupling in reducing the amplitude of the radiated seismic signal from underground nuclear explosions. The first of these tests was SALMON, which was a fully coupled 5.3 kt nuclear explosion conducted at a depth of 828 m on October 22, 1964. This was followed on November 17, 1966 by STERLING HE, a 2.7 ton tamped, high explosive calibration shot which was detonated about 350 m southwest of SALMON at a depth of 831 m. The decoupled nuclear test STERLING had a yield of 0.38 kt and was detonated on December 3, 1966 in the 17 m radius semispherical cavity produced by the SALMON explosion (Perret 1968a,b; Springer *et al.* 1968). Given that the low frequency decoupling factor for STERLING has been estimated to have been approximately 70 ± 20 (Springer *et al.*, 1968), it follows that the amplitudes of the low frequency seismic signals from STERLING were of the same order of magnitude as those to be expected from a 5.4 ton tamped nuclear explosion. It follows that since HE is generally thought to produce low frequency seismic signals which are about twice as large as those produced by a nuclear explosion of comparable energy release, the observed seismic data from STERLING should be directly comparable to that observed from the 2.7 ton STERLING HE explosion. This hypothesis is supported by the fact that the observed seismic amplitude levels at fixed recording stations were generally quite similar for these two events. Thus, these data provide a nearly ideal opportunity to compare seismic data recorded from tamped CE and nuclear cavity decoupled explosions which are nearly co-located and have very similar seismic source strengths.

Although data from STERLING and STERLING HE were recorded at a number of stations located within about 70 km of their common epicenter, the majority of these data are of questionable reliability due to signal-to-noise limitations and other problems. Therefore, in the present analysis we will focus on the stations denoted as 10S and 20S which were located at ranges of 16 and 32 km south of the source locations, respectively (Murphy, 1969). Figures 1 and 2 show comparisons of the vertical component, broadband (1-35 Hz) recordings from STERLING and STERLING HE at stations 10S and 20S. It should be noted that although only these vertical component data will be considered in the following discussion, it has been found that the other components of motion display similar characteristics and, therefore, the conclusions should be considered to be representative of them as well. Figure 1 shows 8 second segments of the recorded time histories at station 10S from STERLING (top) and STERLING HE (bottom). These records are relatively complex for both sources at this near-regional distance, presumably as a result of the propagation path heterogeneities introduced by the source region salt dome structure and the surrounding sedimentary layered sequence which it pierces. Many consistent phases are apparent in the records between the two events. The initial P-wave windows appear to match quite closely for the first second or so. Beginning roughly two seconds after the first arrival is a second phase consisting of a relatively low-frequency carrier with high-frequency signals superimposed. This latter phase produces the largest amplitudes on the vertical component records, and its interpretation is not clear. Springer *et al.* (1968) identified this signal as an S phase, but Gupta *et al.* (1987) determined on the basis of synthetic seismograms derived for a representative structure that this phase arrived too early for S and was more likely reverberating P-waves in the sediments. Accepting this latter interpretation the S-wave window begins about one second later; we follow this interpretation throughout the subsequent discussion. Comparing the signals from the two source types, it can be seen that the most prominent difference is in the ratio of the S to initial P amplitudes, which appears to be on the order of a factor of three larger for STERLING HE than for STERLING.

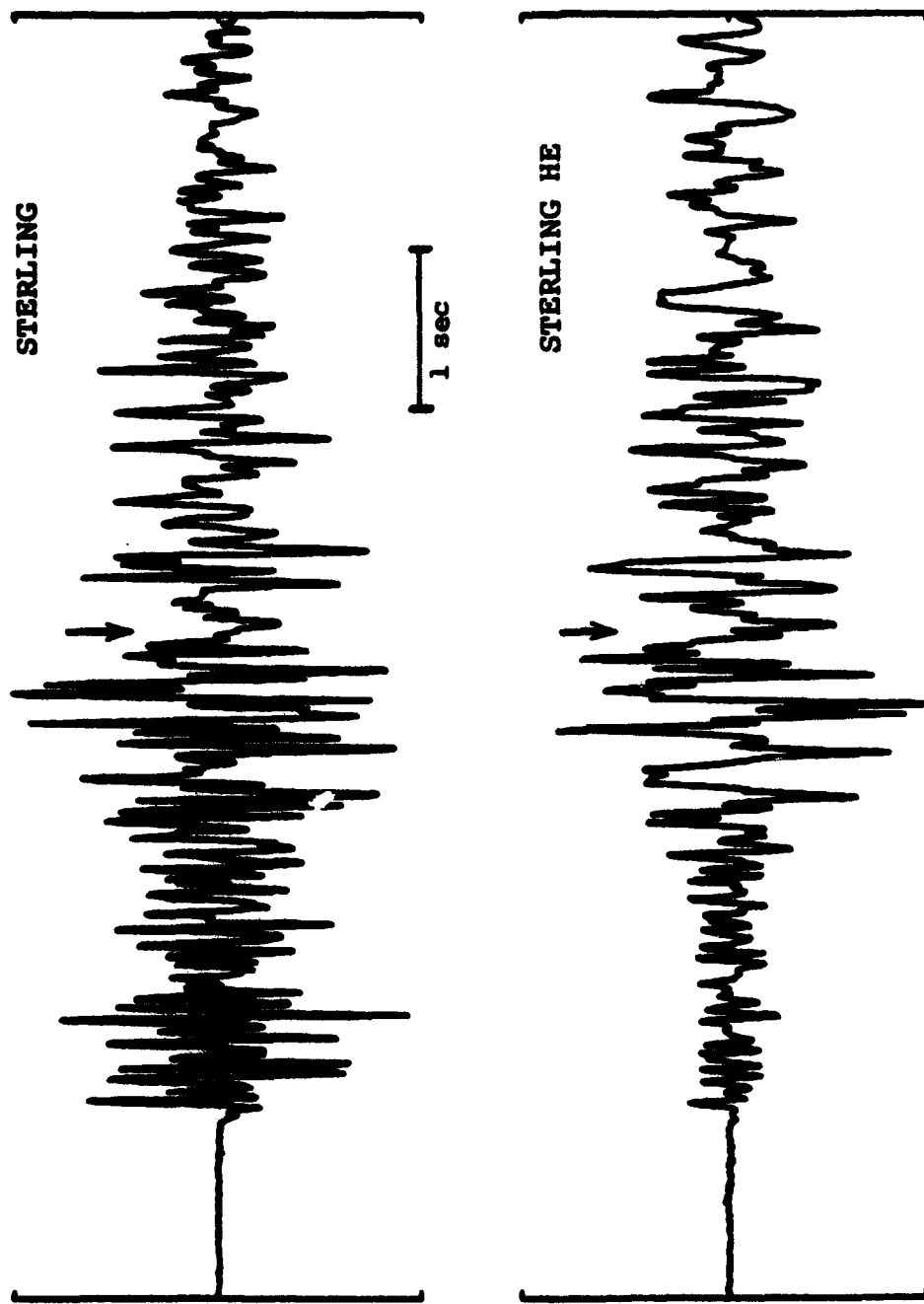


Figure 1. Vertical component time histories at station 10S for STERLING (top) and STERLING HE (bottom). Arrows indicate approximate start of S-wave window.

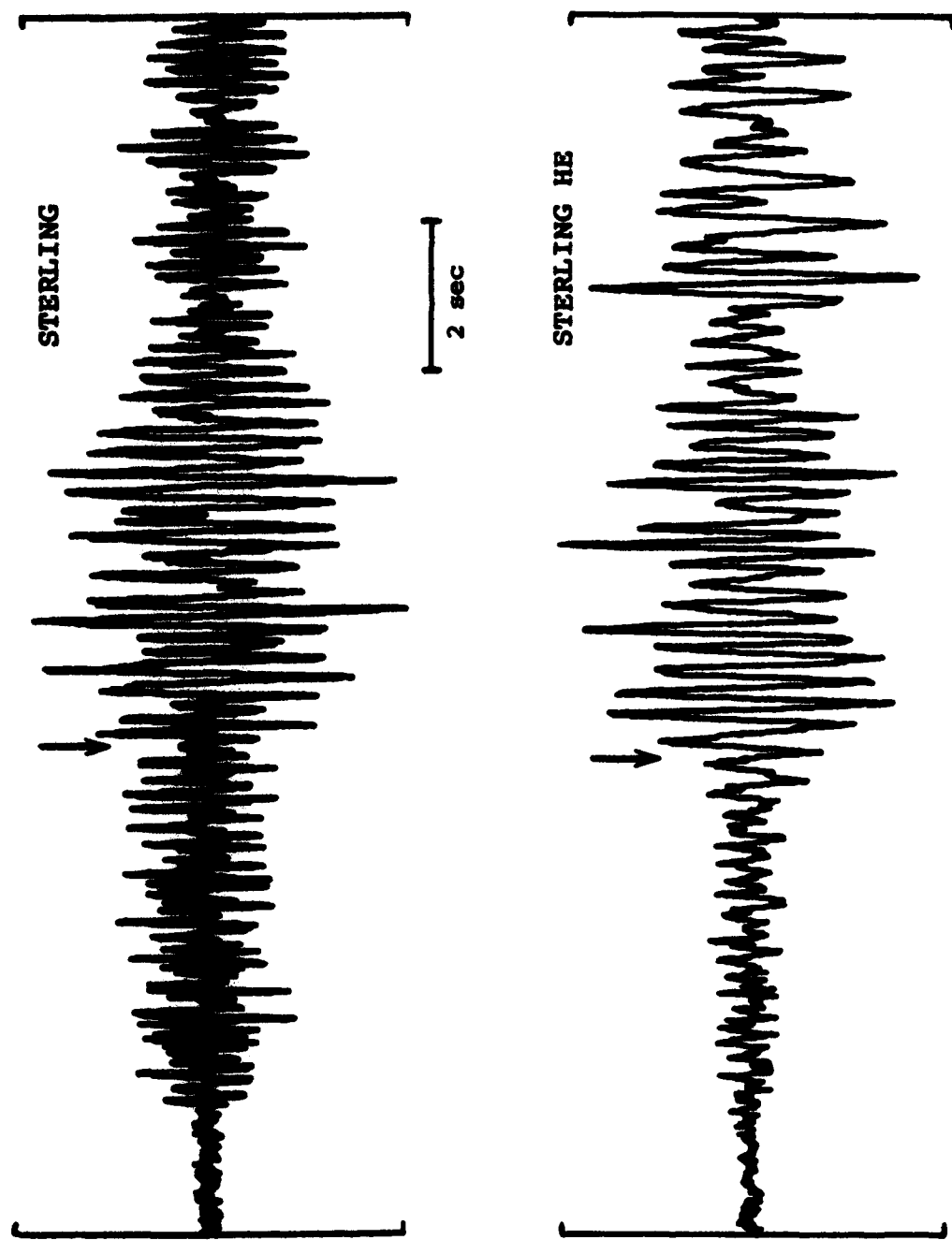


Figure 2. Vertical component time histories at station 20S for STERLING (top) and STERLING HE (bottom). Arrows indicate approximate start of S-wave window.

Similarly, Figure 2 shows 16 second segments of the ground motion time histories recorded at station 20S from STERLING (top) and STERLING HE (bottom). The records are again fairly complex including multiple arrivals in the P-wave window which are apparently associated with the propagation path since we observe general consistency between the two sources. In this case the largest observed amplitudes begin arriving about five seconds after the initial P. This phase is generally lower in frequency and is thought to be S; in this case Gupta *et al.* (1987) agree with the Springer *et al.* (1968) interpretation. Just as for P, the S arrival has a long duration with multiple arrivals apparently associated with propagation in the complex sedimentary structure. Once again, the most prominent difference between these two signals is in the ratio of the S to initial P wave amplitude levels. The difference here is also roughly a factor of three with relatively larger S to P ratios for STERLING HE than for STERLING. Thus, this observation seems to be consistent between stations 10S and 20S.

In an attempt to develop a better understanding of these relative P and S wave differences between STERLING and STERLING HE, spectral analyses were performed on the signals recorded at stations 10S and 20S. Figure 3 shows the initial P wave signal and pre-signal noise spectra determined from the station 10S recordings of STERLING (top) and STERLING HE (bottom). It can be seen from these figures that the P wave spectral amplitude levels are well above the noise levels out to beyond 40 Hz in both cases. Moreover, the signal spectra for the two events appear to be quite comparable with both showing peaks at about 13 Hz, above which they fall off slowly toward higher frequencies. The corresponding P wave signal and noise spectra derived from the station 20S recordings of the two events are shown in Figure 4 where it can be seen that, while the signal-to-noise ratio for STERLING is again good out to about 40 Hz, the STERLING HE signal spectrum is above noise only out to about 25 Hz. In particular, a rather prominent noise spike is apparent in the STERLING HE spectra at about 30 Hz for both signal and noise. Once again, the P wave spectral shapes for the two events appear to be quite similar over the frequency range in which they can be validly compared. These spectra have somewhat

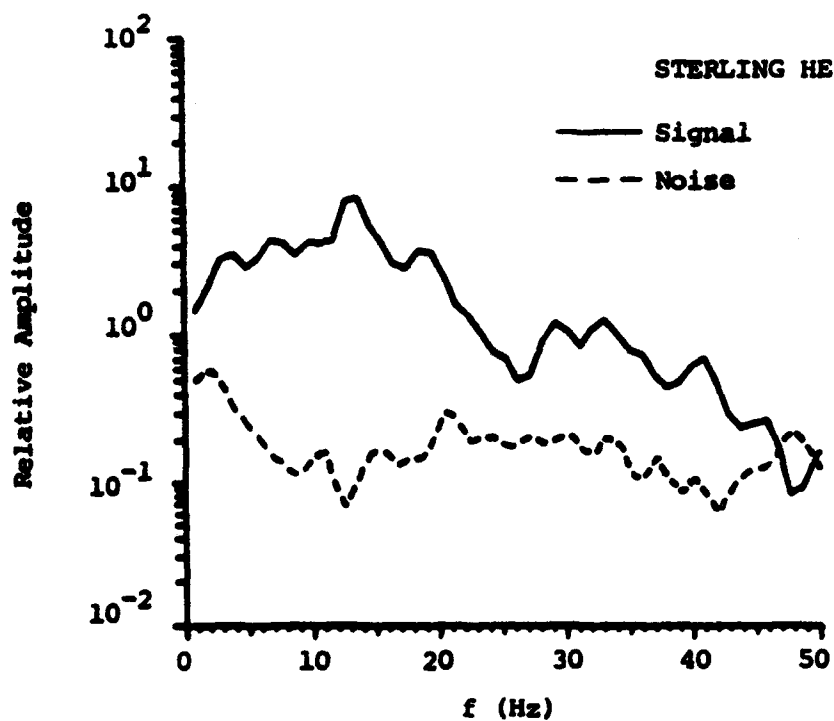
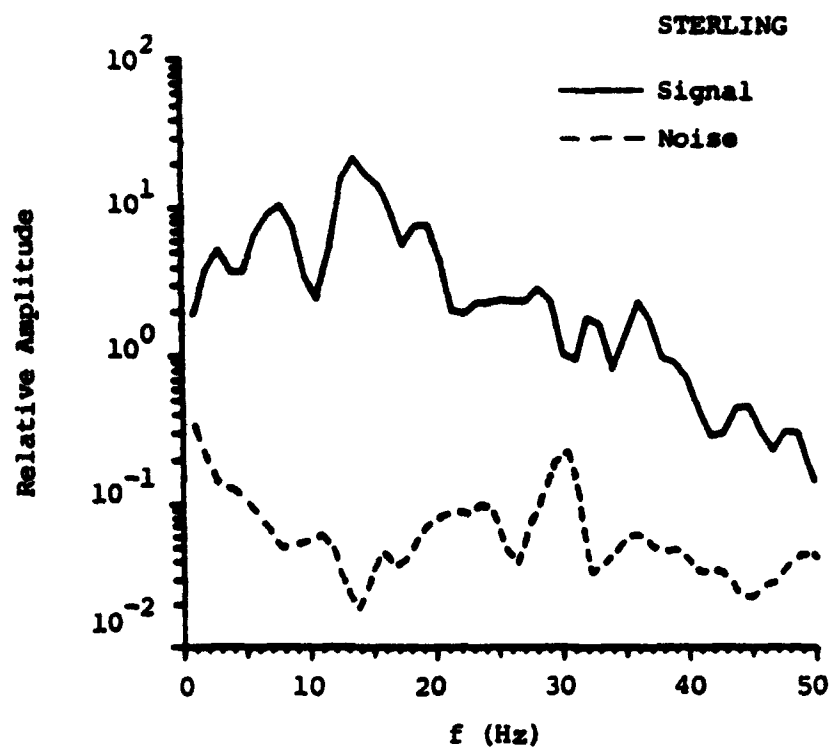


Figure 3. Relative P-wave amplitude spectra at station 10S for STERLING (top) and STERLING HE (bottom).

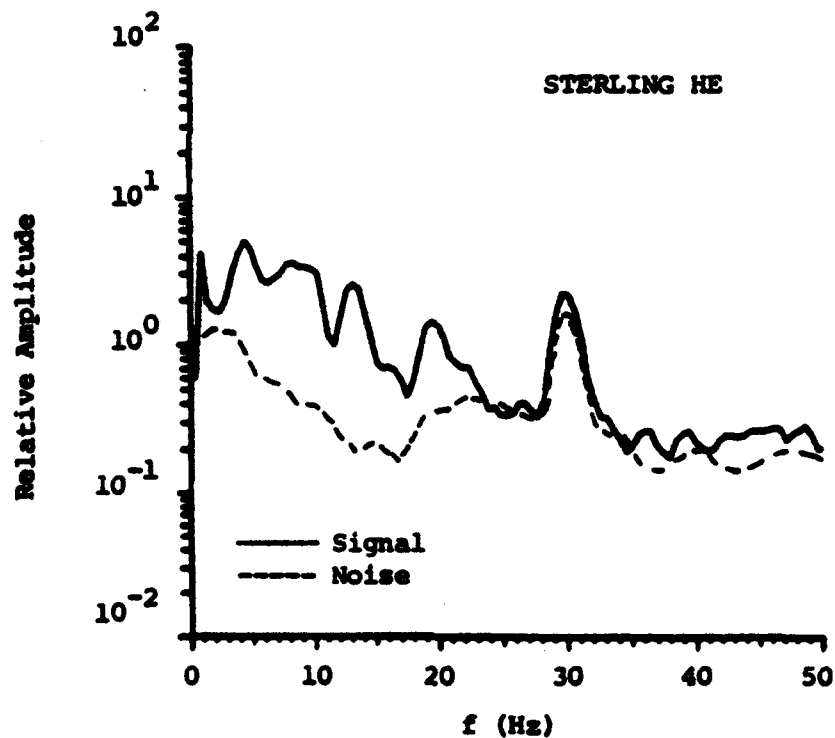
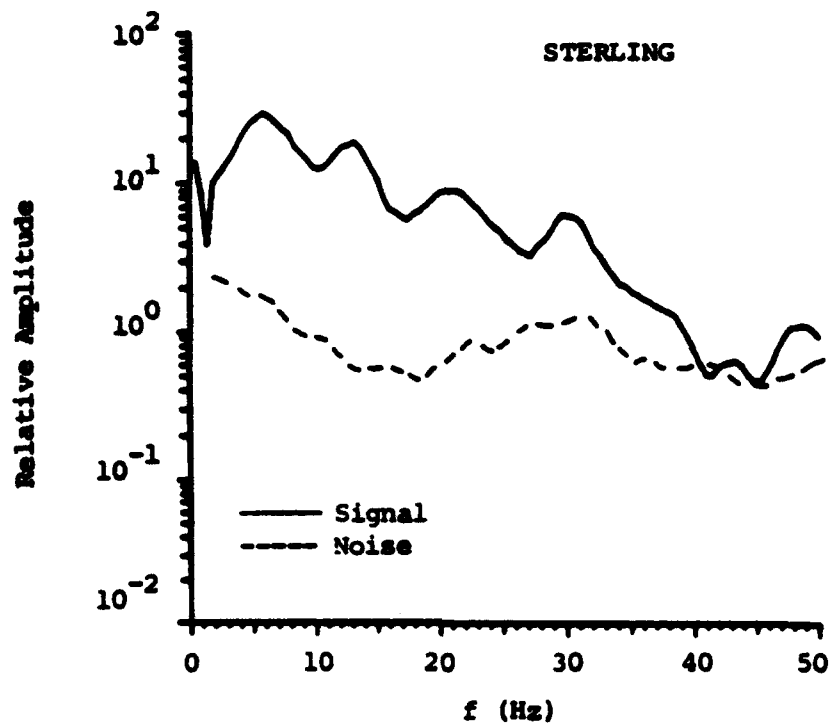


Figure 4. Relative P-wave amplitude spectra at station 20S for STERLING (top) and STERLING HE (bottom).

lower corner frequencies than the corresponding station 10S spectra of Figure 3, presumably due to increased effects of anelastic attenuation on the propagating P wave signals. As a result, the P wave spectra at station 20S have their maximum values at frequencies near 4 to 5 Hz.

The corresponding S wave spectra for STERLING and STERLING HE are plotted in Figure 5 for the signals at station 10S (top) and at station 20S (bottom). At station 10S the signal spectrum is above the noise over the entire frequency band out to 50 Hz for both STERLING and STERLING HE although the STERLING HE signal appears to be close to the noise level at frequencies above about 25 Hz. At station 20S the STERLING S-wave signal spectrum is above noise over the entire frequency range, but the STERLING HE signal drops to the noise level near 25 Hz. For the STERLING HE spectrum the noise spike at 30 Hz, observed in the P-wave results, is again apparent in the S-wave spectrum. At 10S the S-wave spectra for STERLING and STERLING HE exhibit a broad plateau at low frequencies with a corner near 14 Hz; maximum spectral amplitudes are at 9 Hz and 4 Hz, respectively. Comparison of the STERLING and STERLING HE S-wave spectra at station 10S reveals that the STERLING signals are relatively richer in high frequencies above about 5 Hz. At 20S the S-wave spectra show similar behavior. However, at 20S the low-frequency spectral plateau seen at 10S is not apparent; this can again probably be attributed to de-emphasis of the corner by higher attenuation at the more distant station. As a result, the S-wave spectra are observed to decay quite rapidly at frequencies above the spectral peak which is near 5 Hz for STERLING and near 4 Hz for STERLING HE. Again, the spectral decay is less rapid for STERLING so that the S-wave spectra at 20S are enriched at high frequencies relative to STERLING HE. Therefore, at both stations 10S and 20S the decoupled STERLING explosion produced S-waves relatively richer in high frequencies than those from the tamped chemical explosion, STERLING HE.

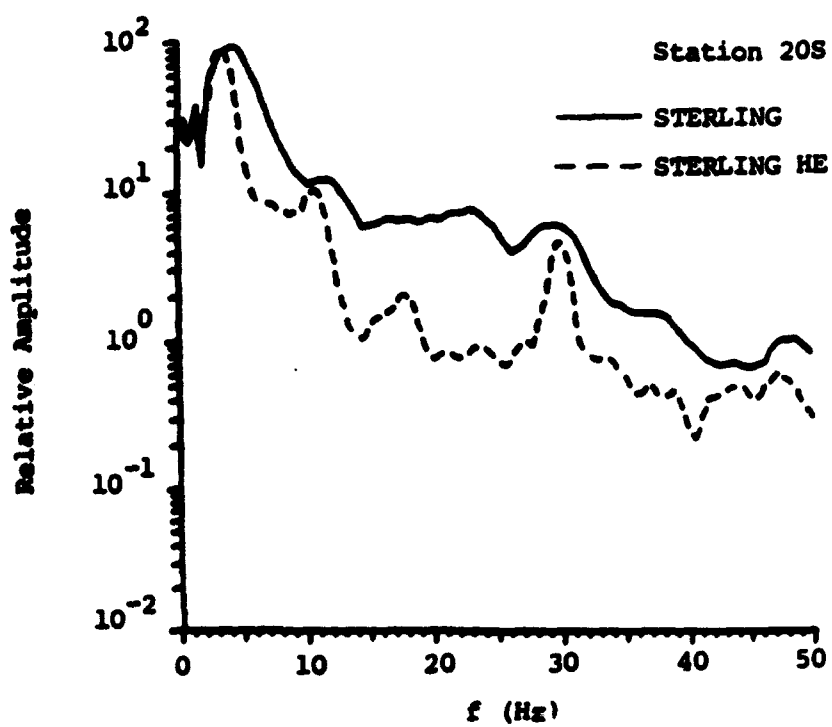
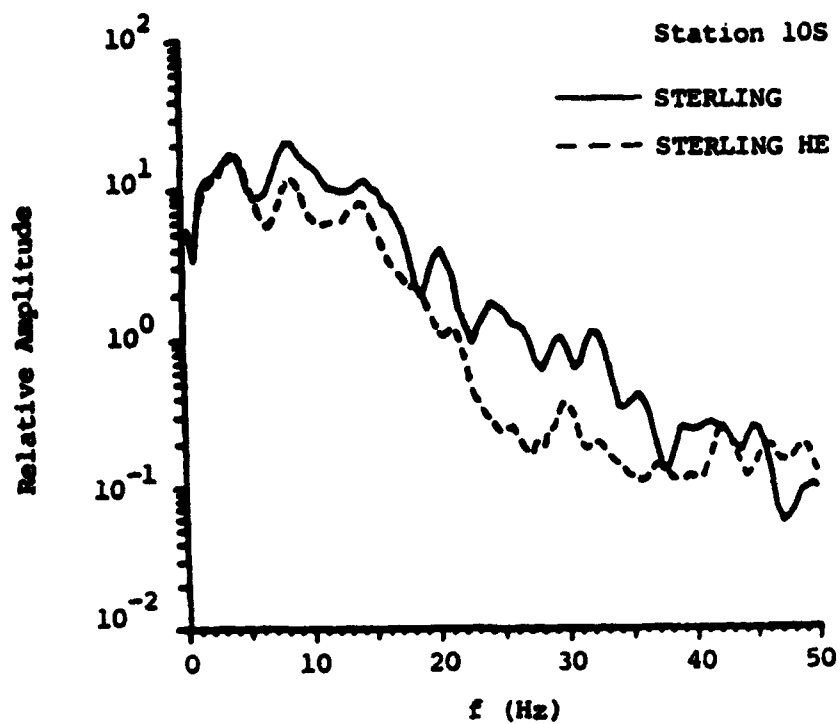


Figure 5. Relative S-wave amplitude spectra from station 10S (top) and 20S (bottom) for STERLING and STERLING HE.

The frequency dependence of the S/P wave ratios for the two source types have also been compared through narrowband filter analyses of the P and S wave signals recorded at stations 10S and 20S. In this approach, the ratio of the maximum amplitudes in the P and S time windows for each filter output are computed and the results are plotted versus the center frequency of the filter. Such ratios are plotted in Figure 6 for station 10S (left) and 20S (right), where the results for STERLING are shown as solid lines and those for STERLING HE as the dashed lines. It can be seen that in all cases the S/P ratios decrease with increasing frequency from maximum values of 3-10 at low frequencies to values on the order of 0.5-1.0 at high frequencies. These results corroborate the previously noted general observations made from the time histories and individual spectra to the effect that the S wave signals are of lower dominant frequency than the corresponding P wave signals at both stations. Of greater potential significance for purposes of event identification, however, is the observation that the S/P ratios are generally about a factor of two larger for STERLING HE than for STERLING over rather broad frequency bands at both stations. At station 10S this difference persists over the entire frequency band out to more than 20 Hz, while at 20S the two ratios are different out to about 12 Hz, above which they appear to converge. However, this apparent high frequency convergence may just reflect the reduced signal-to-noise ratios at higher frequencies at this more distant station. In any case, this large, frequency independent difference in the S/P spectral ratios is generally consistent at the two stations and its persistence over such a broad range of frequencies is a major puzzle. If it could be established that such differences are characteristic of CE and nuclear cavity decoupled explosion sources, then it would be possible to define a valuable new discriminant for use in seismic monitoring. However, before proceeding to such a definition, it is first necessary to establish the physical plausibility and general applicability of any such discriminant. Therefore, it is appropriate to consider the source characteristics and near-source environments of the STERLING and STERLING HE events in greater detail.

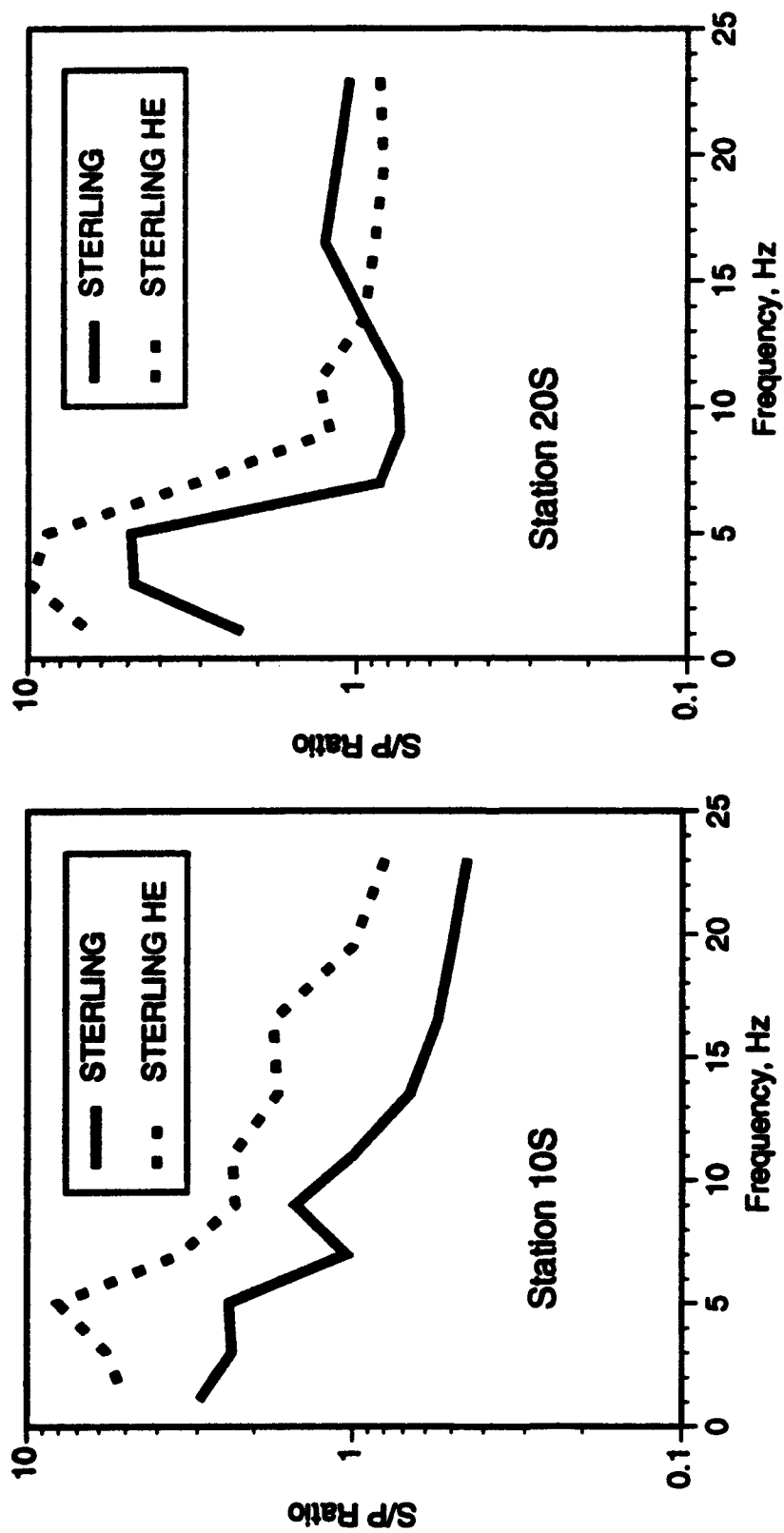


Figure 6. Comparison of S/P amplitude ratios versus frequency for STERLING and STERLING HE determined from narrowband filter analysis of near-regional waveforms recorded at stations 10S (left) and 20S (right).

As was noted previously, STERLING and STERLING HE were detonated at nearly the same depth in the Tatum salt dome with a horizontal separation of about 350 m. Their relative locations with respect to the boundary of the salt dome at source depth are shown in Figure 7 where it can be seen that, while their separation is not negligible with respect to the geometry of the boundary, both shot points are located more than 400 m from the nearest boundary surface. STERLING HE consisted of 2.25 tons of nitromethane which, according to Springer *et al.* (1968), is the energy equivalent of about 2.7 tons of TNT. The explosive was distributed in a circular cylinder with a diameter of 0.99 m and a length of 2.44 m. STERLING, on the other hand, was a 380 ton nuclear explosion in a roughly spherical cavity with a radius of about 17 m. These two source geometries are shown in Figure 8 where they are compared with that of the recent "chemical kiloton" CE test conducted at NTS in September, 1993. It can be seen that none of these initial charge geometries are spherically symmetric and, therefore, the question arises whether such variations in initial source shape could be responsible for the observed differences in S/P ratio between STERLING and STERLING HE. The most direct approach to this problem would be to carry out a nonlinear finite difference simulation of the evolution of the STERLING HE seismic source and then use the results to quantitatively evaluate the relative efficiencies of S and P wave generation by such a source. However, such a detailed simulation analysis lies outside the scope of the current project. Moreover, there is much past experience which suggests that such a simulation would reveal only very minor departures from spherical symmetry in the resulting seismic source function. That is, it has been found that the strong nonlinear response of the medium surrounding the explosion tends to compensate for any asymmetries in the initial charge configuration, producing a much more nearly spherically symmetric seismic source function. Thus, for example, Rimer *et al.* (1993) in their nonlinear simulation of the chemical kiloton charge geometry shown in Figure 8 found that the simulated final cavity volume, cavity pressure and yield radius were virtually identical to the corresponding values computed for a spherically symmetric charge distribution having the same volume.

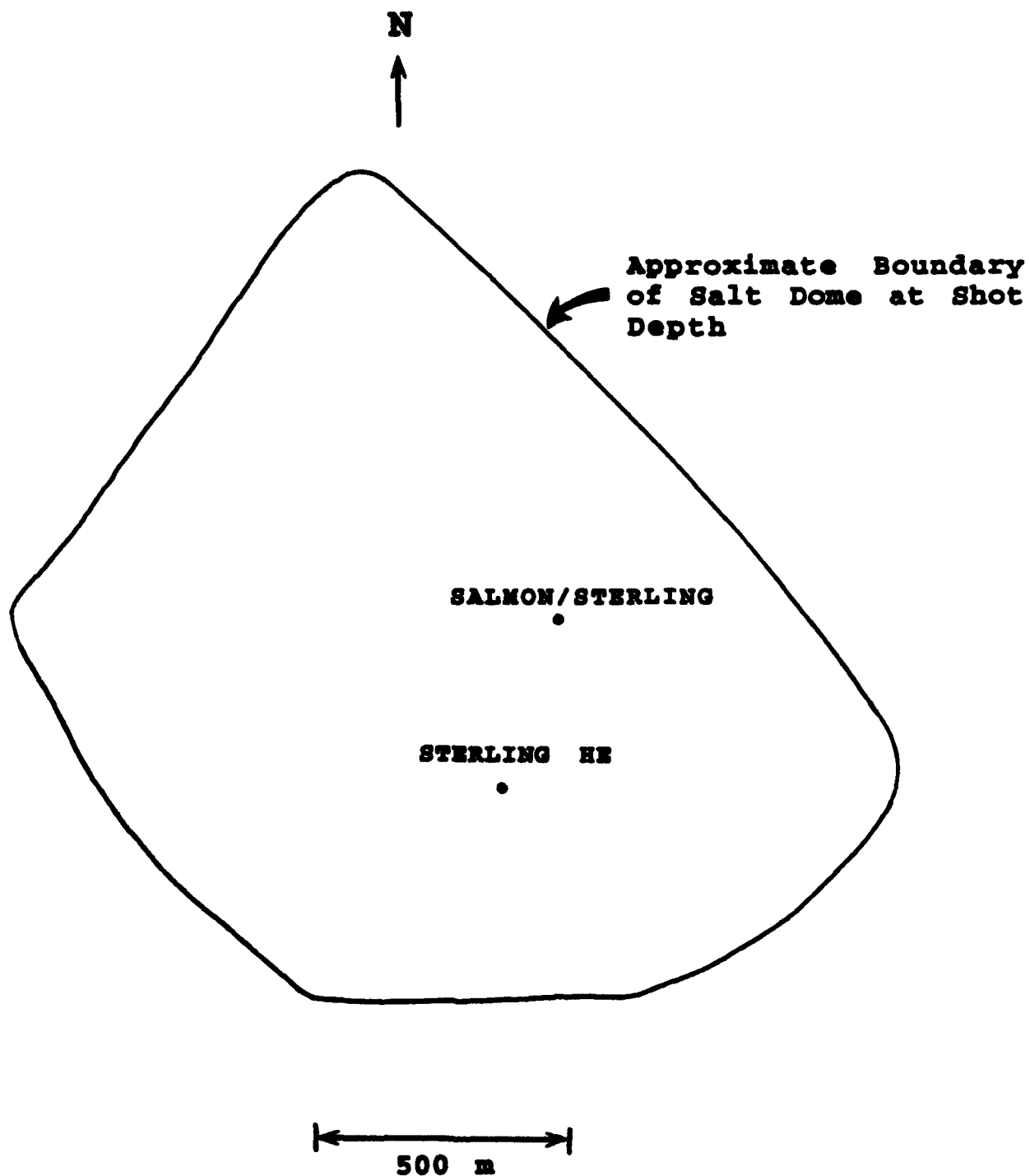


Figure 7. Source locations of STERLING and STERLING HE with respect to the boundary of the Tatum salt dome at source depth.

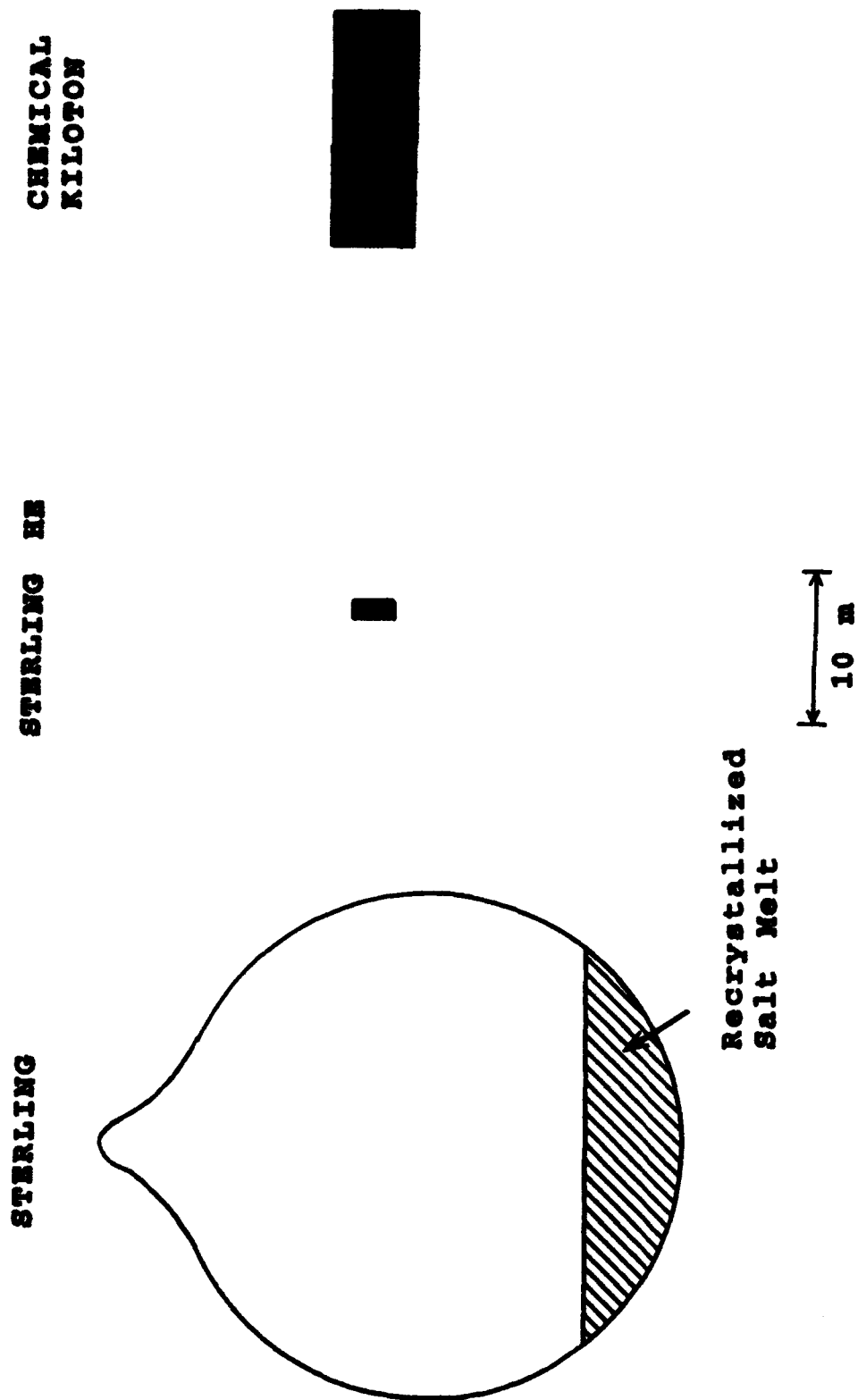


Figure 8. Comparison of initial charge geometries for STERLING, STERLING HE and the NTS chemical kiloton explosion.

Similar results were obtained by Stevens *et al.* (1993) in their simulation analyses of the seismic source functions corresponding to some strongly asymmetric nuclear charge configurations and by Stevens *et al.* (1991) in their simulations of the seismic response of ellipsoidal cavities having much larger aspect ratios than STERLING HE. Therefore, we conclude that it is highly unlikely that the initial charge asymmetry of STERLING HE is responsible for the observed differences in S/P ratios with respect to STERLING.

An alternate possibility is that differences in propagation path characteristics might be responsible for the observed variations in S/P ratios. Thus, although STERLING and STERLING HE were detonated within 350 m of one another in the same salt dome, their positions relative to the dome boundary were somewhat different, as illustrated in Figure 7. Thus, it is possible that the interaction of the outgoing compressional waves with the dome boundaries was different in the two cases, resulting in differences in the P to S conversion efficiency. A remaining difficulty with this hypothesis is that it is not clear why any such boundary effect should be nearly constant over such a broad frequency band. These difficult issues will ultimately have to be addressed using three-dimensional finite difference simulations of the two explosions. In any case, it is probably instructive to note the rather significant seismic differences which can be observed at a common station from similar sources in such close proximity to one another.

In summary, near-regional, broadband seismic data recorded from the STERLING nuclear cavity decoupling test and the nearby STERLING HE tamped CE test have been carefully compared and evaluated for differences which might be diagnostic of source type. It has been demonstrated that although the relative spectral compositions of the P and S waves observed from the two sources appear to be roughly comparable, the S/P spectral ratios are significantly different over a broad frequency band extending from at least 1 to 10 Hz. Evaluation of the possible effects of differences in initial charge geometry have been evaluated in a preliminary fashion and it has been concluded that it is unlikely that such effects can explain the

observed differences in S/P ratios in this case. An examination of the potential influence of variations in the locations of the two explosions with respect to the boundaries of the Tatum salt dome suggests that this might be a contributing factor, although it is not clear at this time that such a mechanism can explain the frequency independent nature of the observed seismic differences. In conclusion, additional experimental data will have to be evaluated before it can be determined whether observed seismic differences of the kinds noted for STERLING and STERLING HE can be used to reliably discriminate between tamped CE and nuclear cavity decoupled explosions.

3. Comparison of P Wave Signals Recorded at NORSAR from CE and Nuclear Cavity Explosions in the North Caspian Basin

The area surrounding the Caspian Sea provides a good test bed for evaluating procedures for identifying cavity decoupled nuclear explosions in that it contains the Azgir test site at which the Russians have acknowledged conducting a number of nuclear explosions in salt cavities. Moreover, although the natural seismicity of the area surrounding the Azgir site appears to be quite low, there appear to be significant numbers of CE events occurring in the salt dome regions of the North Caspian Basin which can serve as a source of seismic data to be compared with corresponding data from nuclear cavity explosions for evaluation of potential discriminants. In the following discussion, we will first briefly review the seismicity of the Caspian region and then proceed to a comparison of NORSAR P wave data recorded from selected CE and nuclear cavity explosions in the North Caspian Basin.

Strong differences in tectonics and natural seismicity exist in the region surrounding the Caspian Sea. The southern region, including the Caucasus mountains west of the Caspian and the Kopet Dagh area east of the Caspian, is tectonically active with a high level of natural earthquake activity. In contrast the northern Caspian basin is a stable platform region with little, if any, natural seismicity. This dichotomy is illustrated in Figure 9 which depicts epicenters of earthquakes with energy class $K > 11$ ($m_b > 4$) reported in the annual Russian earthquake catalogs for the period 1962 to 1979. The earthquake activity tends to be clustered, but the map shows a clear diminution in the level of seismicity north of about 44° latitude on the west side of the Caspian and a similar drop off in activity north of 40° latitude on the east side of the Caspian. Although this northward drop in seismicity may to some extent reflect Russian reporting practice and bias associated with the locations of Soviet seismograph stations, the stable

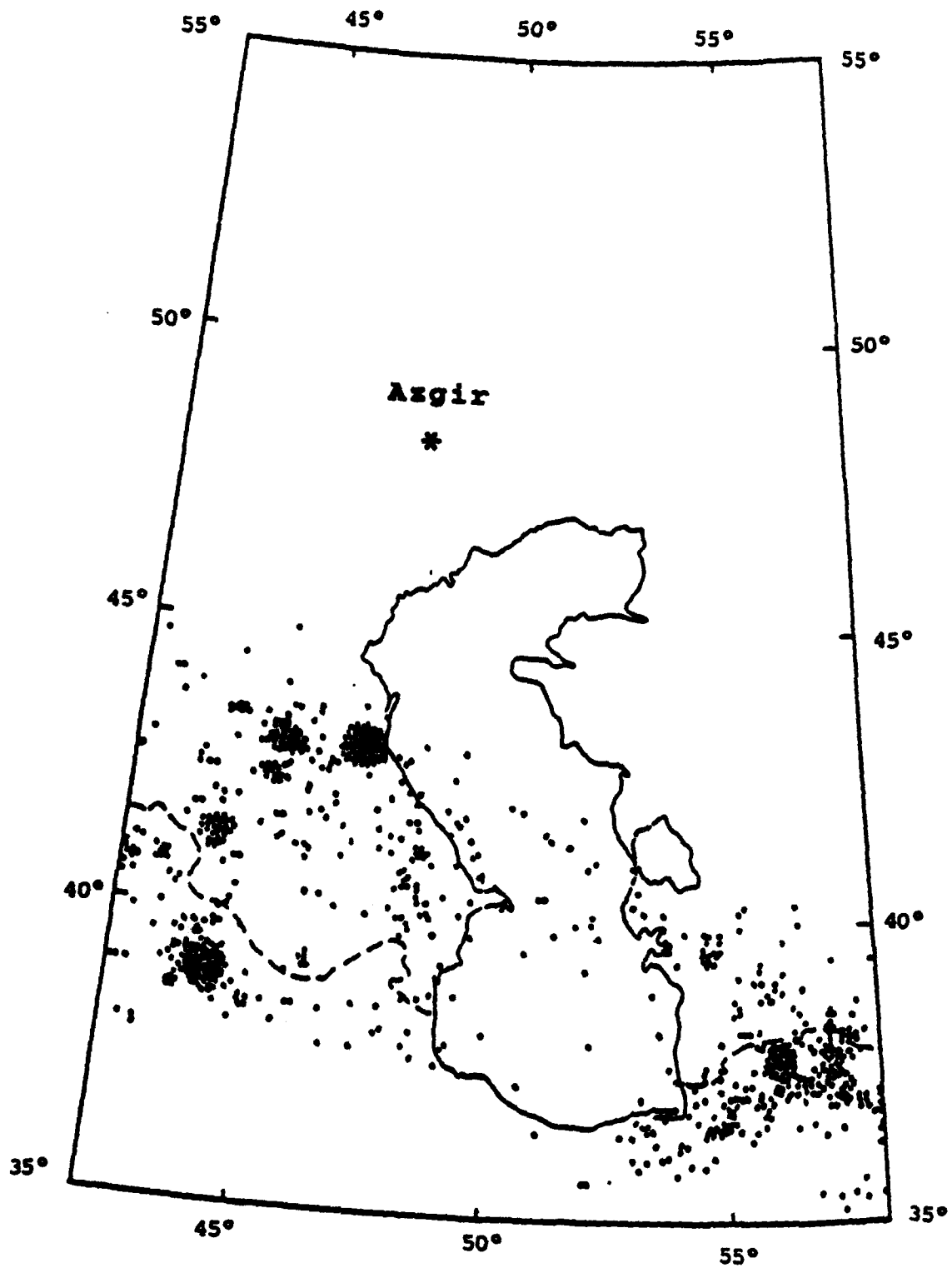


Figure 9. Epicenters of earthquakes with $K > 11$ in the Caspian region developed from Russian earthquake catalogs for the period 1962 to 1979.

geologic conditions and total absence of earthquakes in the northern Caspian basin as reported in international catalogs appears to confirm that the area is seismically quiet. This is potentially significant in the current context, since the principal Soviet nuclear testing area in salt was located in the northern Caspian basin at Azgir (cf. Figure 9). Thus, this region provides a prototype for the environment in which seismic monitoring for cavity decoupled explosions might take place.

At first glance, the results summarized in Figure 9 might suggest that detection of a seismic event in the vicinity of Azgir is equivalent to its identification as a nuclear explosion. However, even though this region seems to be largely devoid of natural earthquake activity, a number of low level seismic events are in fact detected in the area every year. For example, Ringdal (personal communication, 1984) has identified more than 180 events in the NORSAR catalog which were located in the aseismic area bounded by 45°N and 52°N north latitude and by 42°E and 55°E longitude during the time period October, 1971 to October, 1981. The NORSAR locations for these events are shown in Figure 10 where it can be seen that they completely surround the Azgir nuclear testing area. Ringdal has concluded that most of these events are probably chemical explosions on the basis of their strong clustering during the local daylight hours. This fact is illustrated in Figure 11 which shows a comparison of the distribution of times of occurrence of the seismic events from Ringdal's north Caspian list with that for natural earthquakes from the Caucasus area to the south. It can be seen that the north Caspian events from the NORSAR list are strongly clustered in the time period from about 6 to 18 hours GMT, in contrast to the Caucasus events which seem to be evenly spread throughout the 24 hour period. This strong peaking of the events from the NORSAR list suggests that the majority of them are not natural. Given this observation and the presence of oil-shale development and construction activities in the area, it seems reasonable to conclude that these events are mostly chemical explosions similar to those which might be found in other seismically quiet areas of the world.

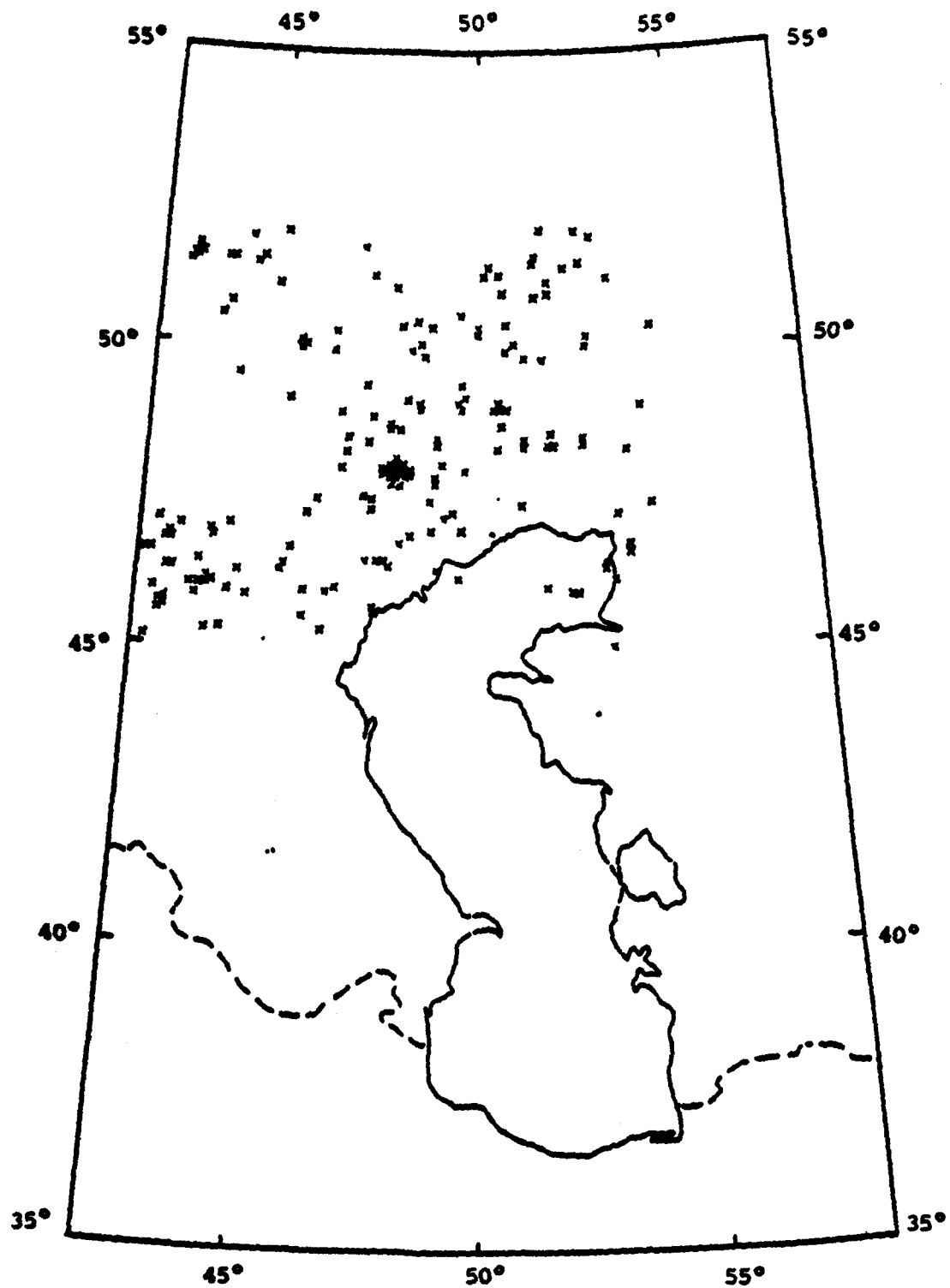


Figure 10. Locations of events reported by NORSAR for the aseismic area bounded by 45°N and 52°N and by 42°E and 55°E during the time period from October, 1971 to October, 1981.

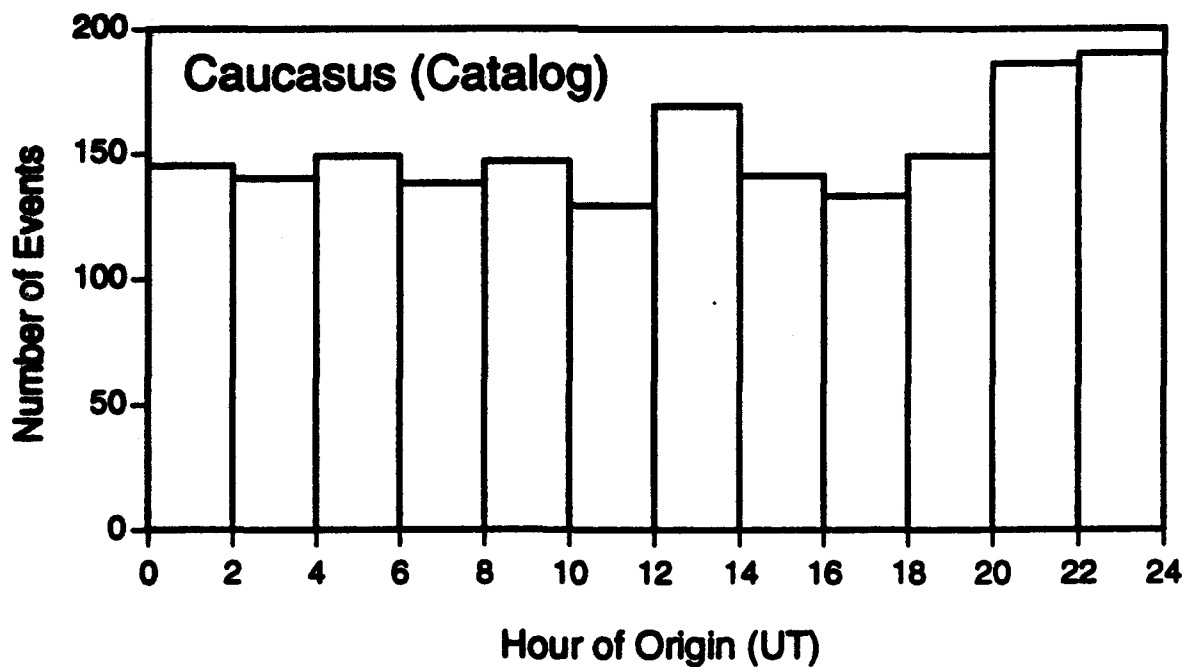
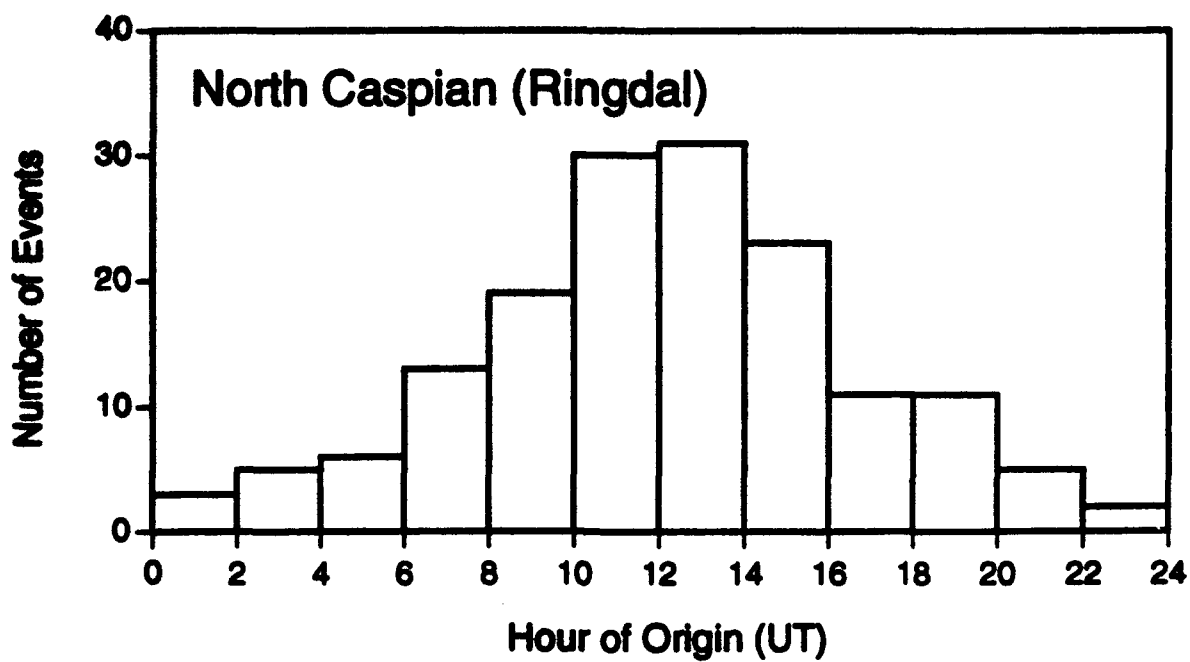


Figure 11. Comparison of the distribution of times of occurrence of the seismic events from Ringdal's north Caspian list (top) with that for natural earthquakes from the Caucasus area to the south (bottom).

As was indicated above, a number of North Caspian nuclear and presumed CE events have been detected by the NORSAR array and listed in the NORSAR event bulletin. Table 1 lists the sample of 12 such events which have been selected for comparative analysis. It can be seen that the first eight of these have been designated as presumed CE events, while the last four have been identified by the Russians as having been nuclear explosions in salt cavities at Azgir (Sultanov, personal communication, 1993). It can be seen that the NORSAR m_b estimates listed in this table indicate that the samples for the two source types encompass about the same range in magnitude, thereby permitting direct comparisons of the recorded seismic data. The NORSAR locations of these selected events are plotted on the map of the North Caspian region in Figure 12 where it can be seen that the estimated locations of the presumed CE events surround the locations of the nuclear explosions. Note from Table 1 and Figure 12 that Events #1 - #3 appear to be co-located and were detonated on the same day at intervals of about 14 seconds, which would seem to confirm that at least these three are CE events. It is difficult to assess the accuracy of the NORSAR locations given the available information, but, given the size of the events and their distance from NORSAR ($\Delta \sim 25^\circ$), it would not be surprising if the epicentral uncertainties are on the order of 100 km or more. This rough estimate agrees with the observed maximum mislocation of the Azgir nuclear explosions, which is on the order of 125 km for Event #12.

With regard to the nuclear explosions, the Russians have confirmed that explosions #9 - #12 in Table 1 were detonated in two different cavities in salt at the Azgir test site. More specifically, Adushkin *et al.* (1992) have indicated that Event #9 was an 8 kt decoupled nuclear test conducted in the 38 m radius, air-filled cavity produced by the 64 kt tamped nuclear explosion conducted at Azgir on 12/22/71. Similarly, Sultanov *et al.* (personal communication, 1993) report that Events #10 - #12 were sub-kiloton nuclear tests conducted in the 32 m radius, water-filled cavity produced by the 25 kt tamped nuclear explosion of 7/1/68. Thus, only Event #9 was a true decoupling test and even that was only partially decoupled as a result of the fact that its yield was a factor of three or more larger than that

Table 1.
NORSAR Source Parameters of Selected
North Caspian Events

Event #*	Date	Origin Time (UT)	N Lat.	E Long.	mb
1 (CE)	09/14/78	04:00:02	51.2	53.2	3.6
2 (CE)	09/14/78	04:00:16	51.2	53.2	3.6
3 (CE)	09/14/78	04:00:29	51.2	53.2	3.6
4 (CE)	04/28/84	14:53:48	46.2	45.8	4.5
5 (CE)	06/27/86	07:25:44	48.1	48.7	4.1
6 (CE)	07/25/86	07:22:35	47.4	49.9	3.9
7 (CE)	08/22/86	06:31:37	48.3	49.4	4.0
8 (CE)	09/28/86	14:08:16	45.6	47.5	4.4
9 (NC)	03/29/76	07:00:03	48.0	48.0	3.9
10 (NC)	10/14/77	07:00:02	48.0	48.0	3.9
11 (NC)	09/12/78	05:00:01	48.0	48.0	3.5
12 (NC)	01/10/79	07:59:53	46.9	48.3	4.1

* CE denotes presumed chemical explosion and NC denotes nuclear cavity test.

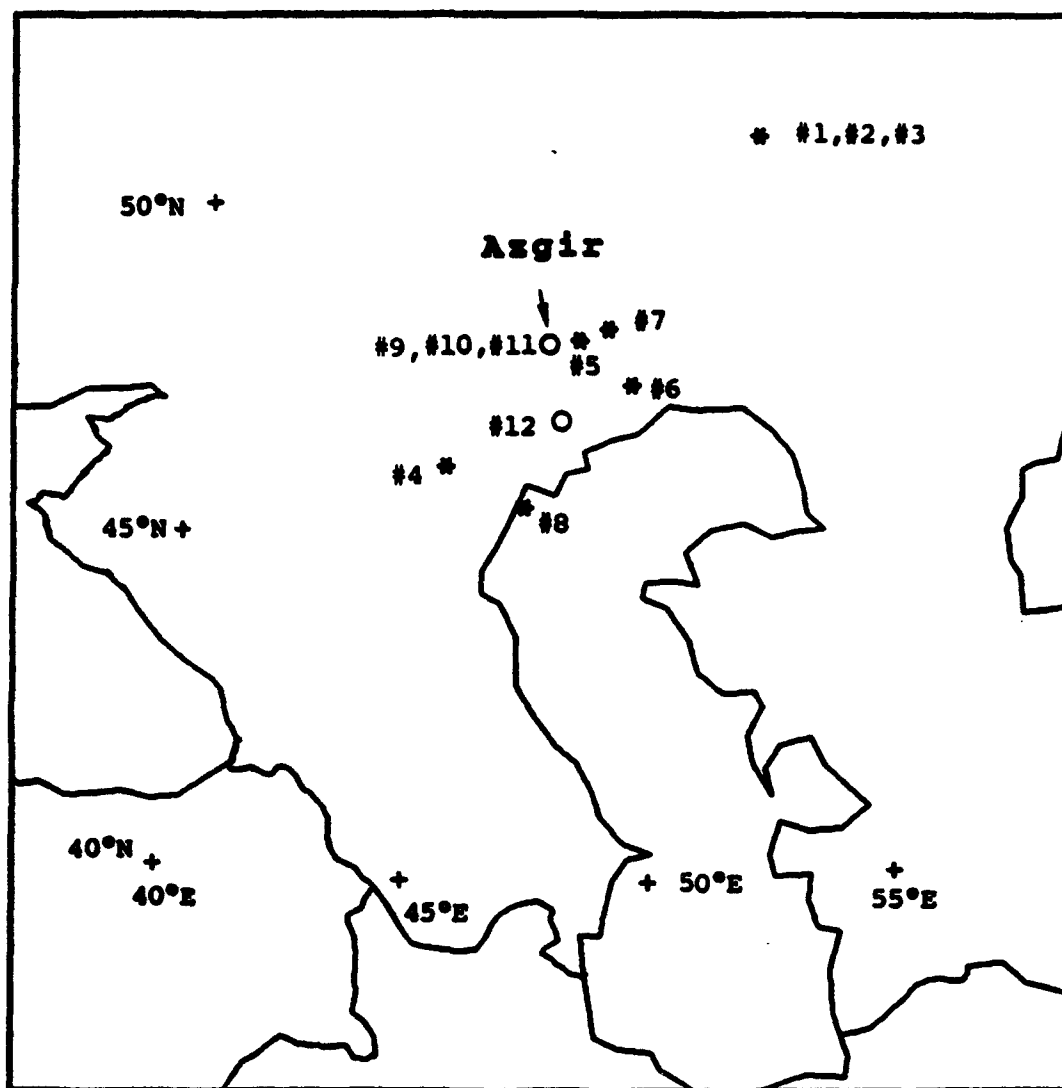


Figure 12. NOR SAR locations of the selected Caspian events. Open circles denote nuclear cavity tests while asterisks denote presumed chemical explosions.

specified by the Latter criterion for full decoupling in a cavity of that size. Moreover, the water-filled cavity tests were observed to have coupled better than tamped explosions of the same yield in salt, consistent with previous experience of the relative seismic coupling efficiency of nuclear explosions in water. However, all four of these nuclear tests were conducted in nearly spherical cavities in salt and, therefore, except for absolute amplitude level, they might be expected to produce low frequency seismic signatures comparable to those expected from fully decoupled nuclear explosions.

Full NORSAR array data have been retrieved for each of the 12 events of Table 1 and previewed to assess relative data quality across the array. In agreement with the results of previous studies by Ringdal *et al.* (1983), it was found that subarray O2B consistently provides the highest quality signals for these north Caspian events and, consequently, our analyses have focused on data recorded at the six elements of this subarray. The recordings at the center element (i.e., O2B0) for the 12 selected events are compared in Figure 13. It can be seen that the signal-to-noise ratios at this station are generally quite good for these events, although there is some evident interference from longer period microseismic noise. Due to the differences in relative frequency content, this noise can be effectively suppressed by filtering and Figure 14 shows the results of filtering the seismograms of Figure 13 through a bandpass filter with corner frequencies at 0.8 and 6.0 Hz. It is evident from these figures that there are some significant differences in the short-period P waves produced by these events. For example, the recordings from the HE Events #4, #5 and #6 are more emergent and have higher coda levels than those of the nuclear cavity Events #9 - #12, which are very similar to one another. On the other hand, the recordings from some of the HE Events (e.g., #1 - #3) appear to be quite similar in character to the nuclear recordings. Thus, in terms of general time domain characteristics, the recordings from the presumed chemical explosions show a degree of variability which appears to encompass the characteristics of the corresponding decoupled seismograms.

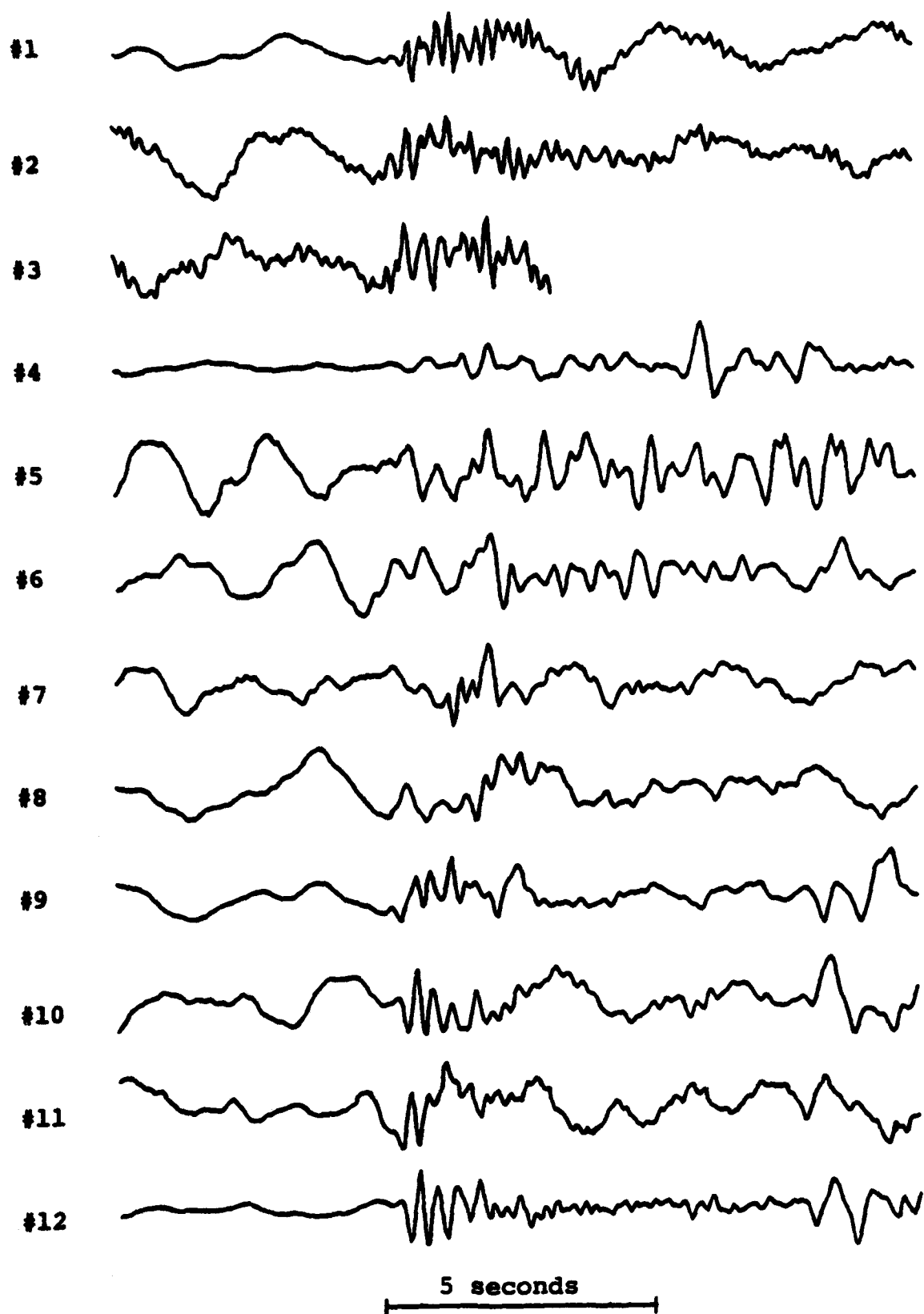


Figure 13. NORSAR subarray element O2B0 recordings of selected Caspian seismic events.

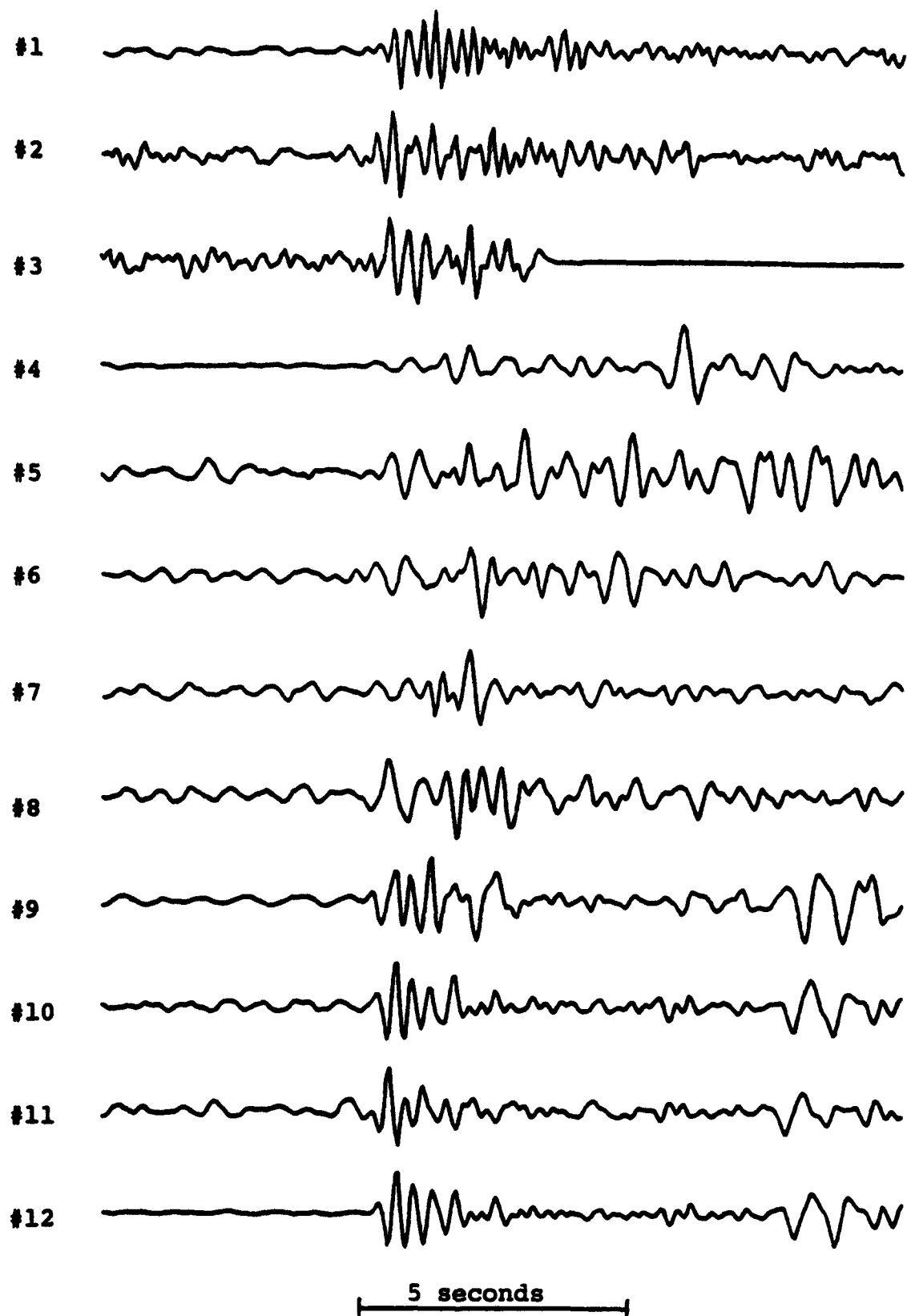


Figure 14. Filtered (0.8-6.0 Hz) NORSEAR subarray element O2B0 recordings of selected Caspian events.

The next step in the analysis procedure was to estimate P wave signal and noise spectra for the 12 events at each of the six elements of subarray O2B. The data were recorded at a sampling rate of 20 samples/second and the spectra were computed using the first 4.5 seconds of the P wave signal and a corresponding window of pre-signal noise. The resulting spectra were smoothed and corrected for instrument response and representative spectra for Events #1, #4 and #10 are displayed in Figures 15, 16, and 17, respectively. With reference to Figures 15-17, it can be seen that the usable passband generally extends from about 1-2 Hz to about 7-9 Hz. Although there is some evidence of site effects on the spectra observed at the individual elements, the P wave spectral composition has been found to be quite stable across the O2B subarray. This is illustrated in Figures 18-20 which show the individual element and subarray-averaged P wave spectra corresponding to the events of Figures 15-17, plotted over the passbands containing usable signal-to-noise ratios. The dashed lines enveloping the subarray averages in these figures denote the one standard error of estimate levels which, for the six element array, correspond roughly to 95 percent confidence intervals about the average values. For the HE events exemplified by Figures 18 and 19, the standard error of estimate over this frequency band averages to less than a factor of 1.5. Somewhat surprisingly, the variation in P wave spectra across the subarray appears to be noticeably larger for the nuclear cavity explosions, averaging to nearly a factor of 2.0, as illustrated in Figure 20. There is no obvious reason for this difference and it may just reflect the fact that the decoupled events are generally older and may have been recorded during a period in which the instrument calibration factors were less well determined than they have been in more recent times.

Examination of these subarray-averaged P wave spectra indicates that the events can be roughly divided into three groups, consisting of Events #1 - #3, Events #4 - #8 and the nuclear cavity Events #9 - #12. The subarray-averaged spectra within each of these three groups are compared in Figures 21-23, respectively, where the individual spectra have been normalized to

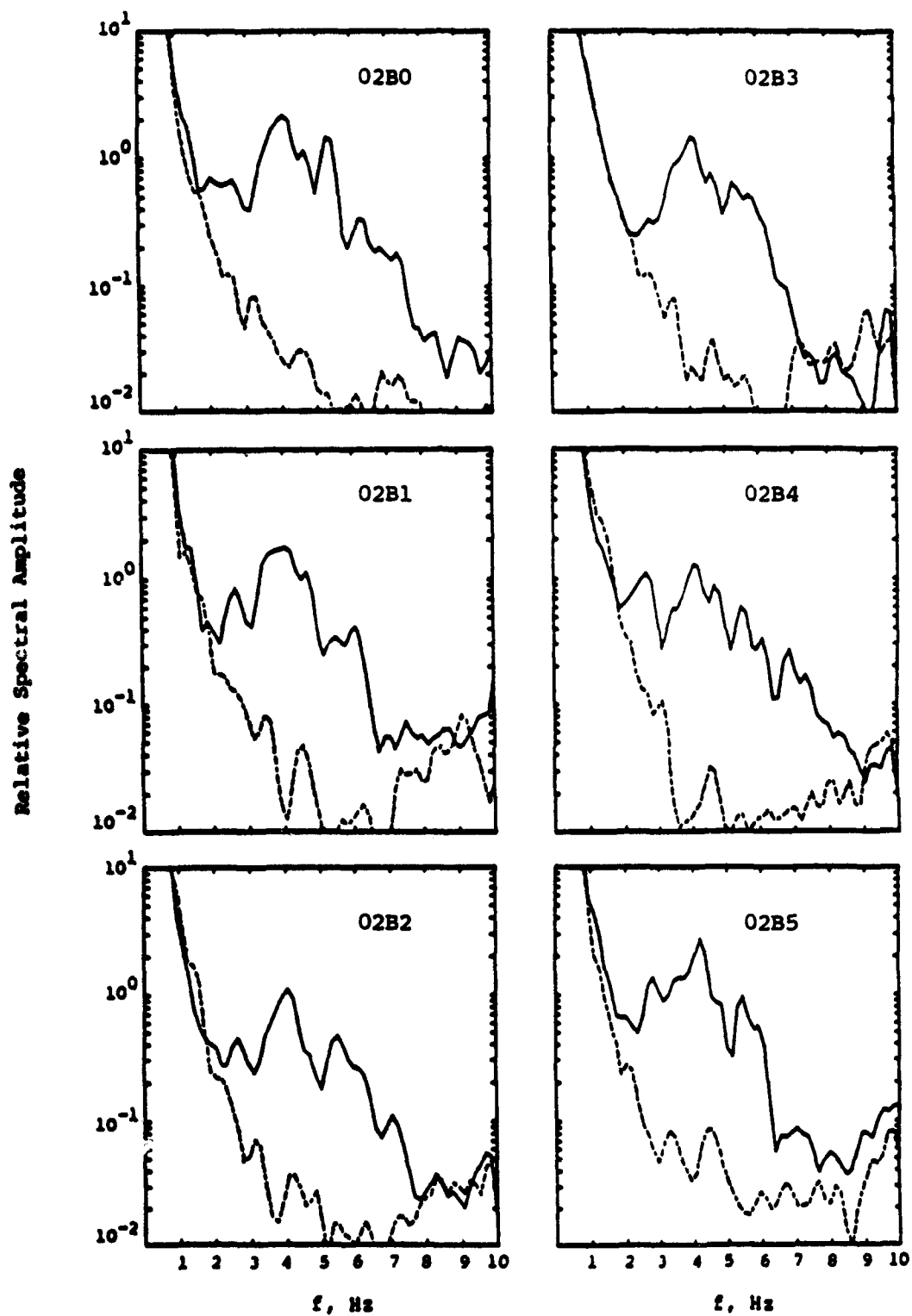


Figure 15. NOR SAR subarray O2B P wave signal (solid line) and noise (dashed line) spectra for Event #1.

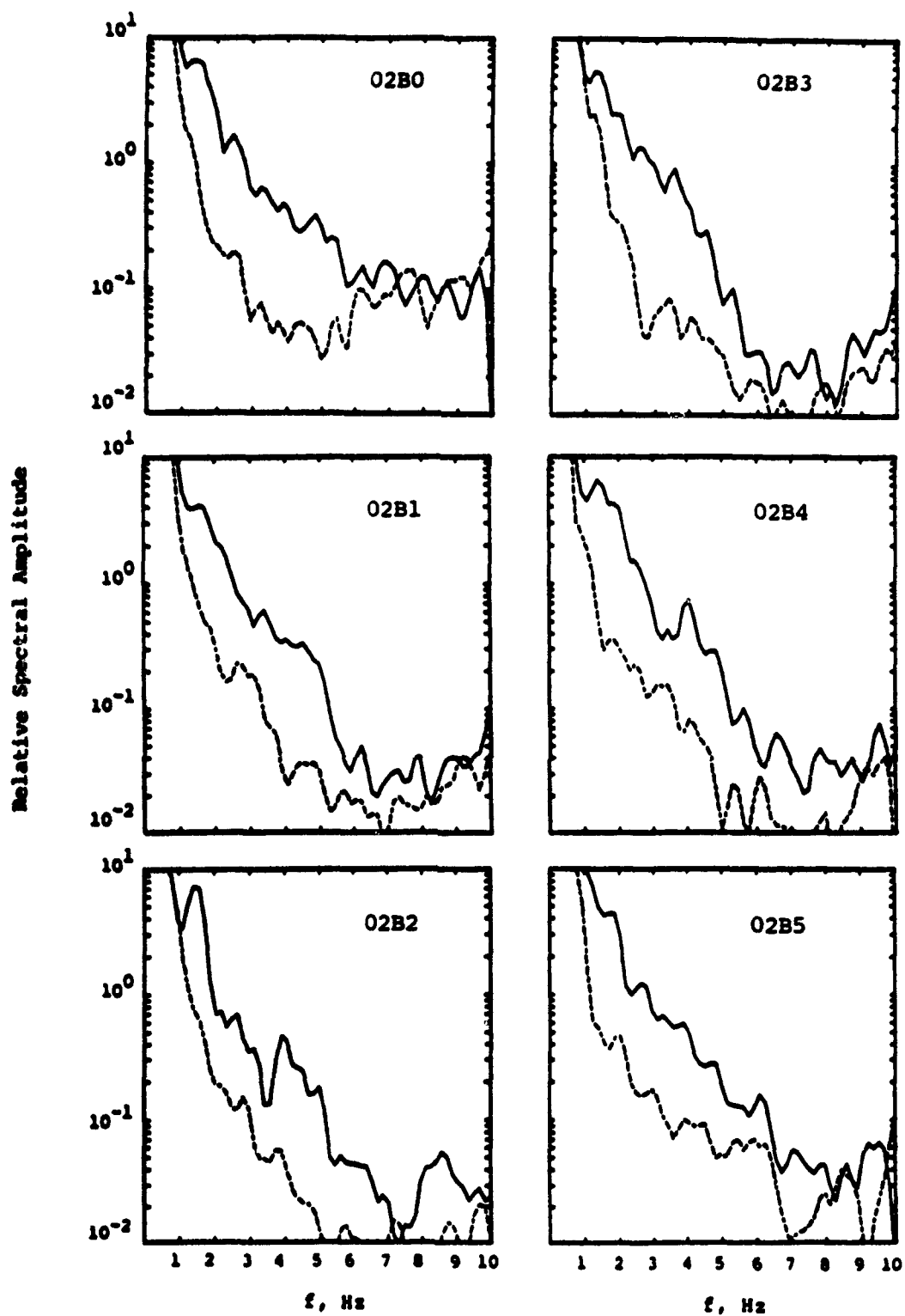


Figure 16. NORSAR subarray O2B P wave signal (solid line) and noise (dashed line) spectra for Event #4.

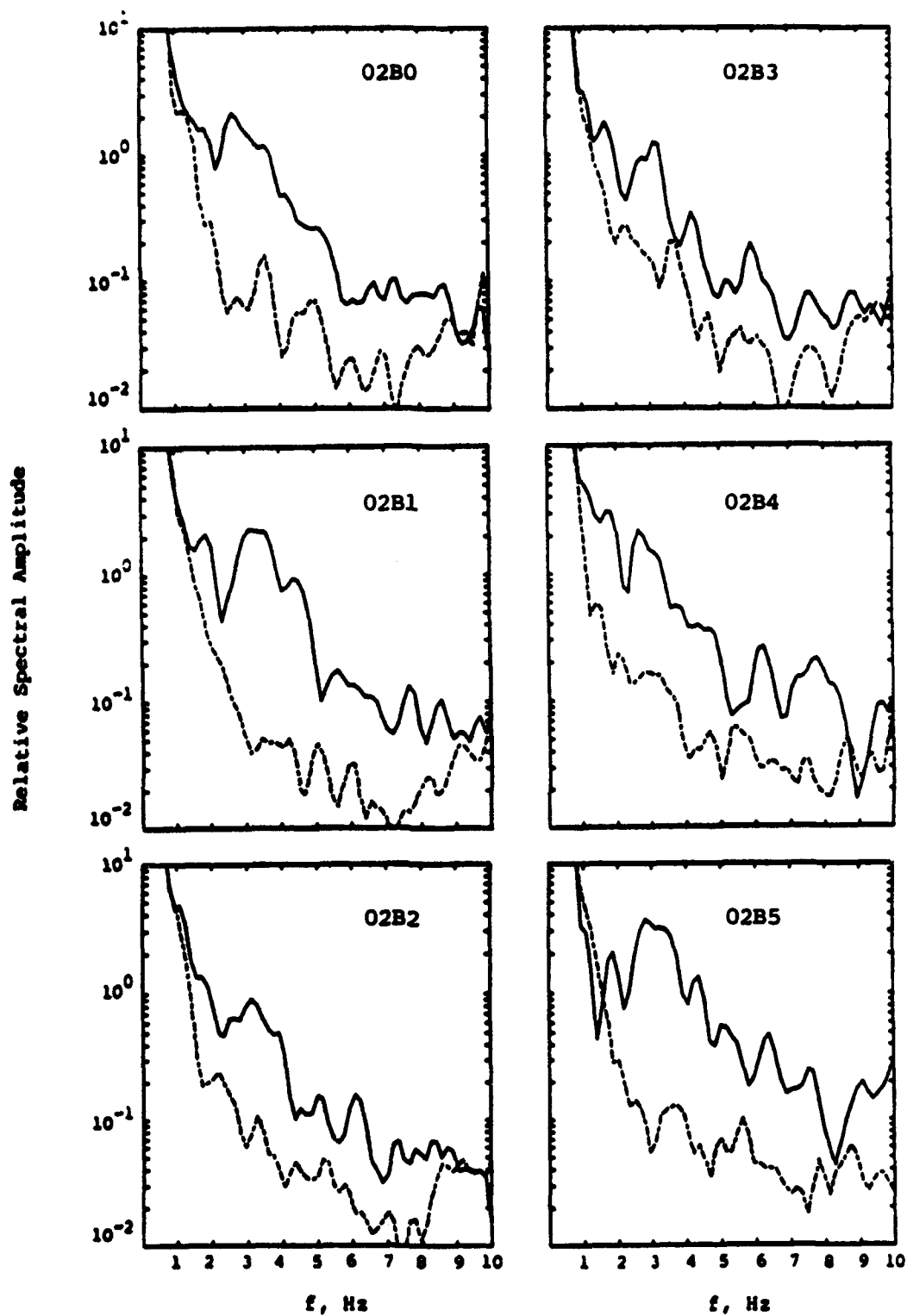


Figure 17. NOR SAR subarray O2B P wave signal (solid line) and noise (dashed line) spectra for Event #10.

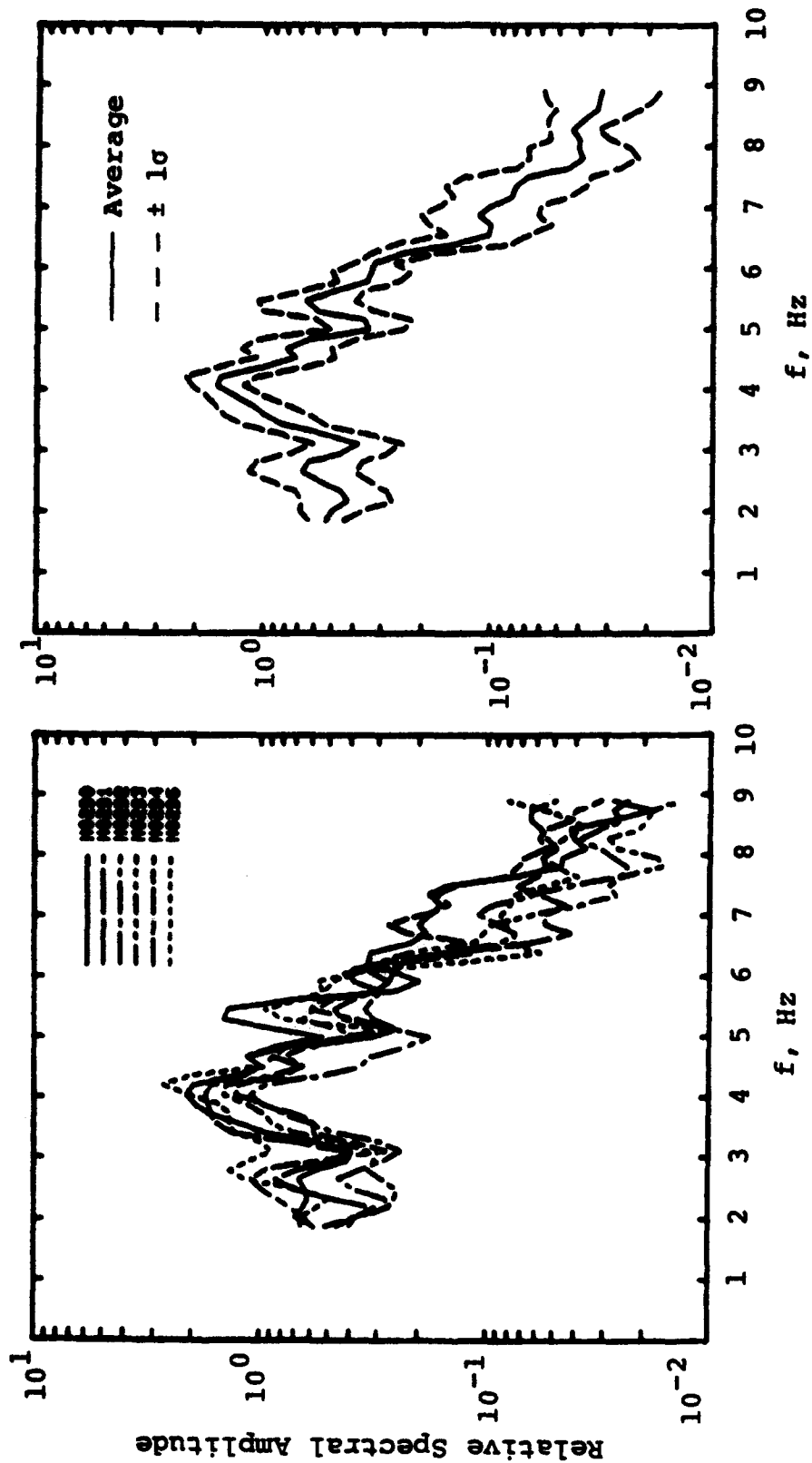


Figure 18. NORSAR O2B single element (left) and subarray-averaged (right) P wave spectra for Event #1.

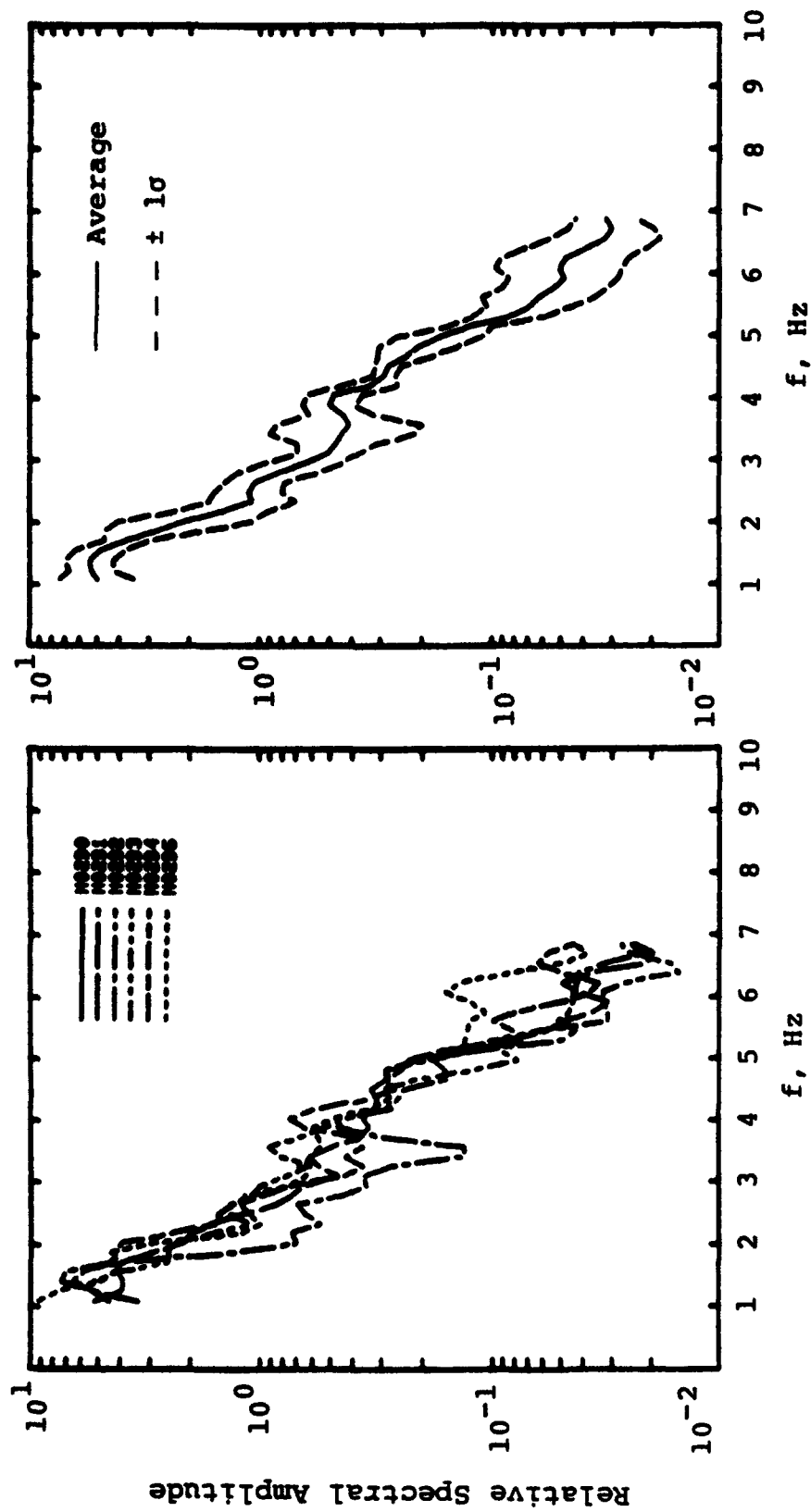


Figure 19. NOR SAR O2B single element (left) and subarray-averaged (right) P wave spectra for Event #4.

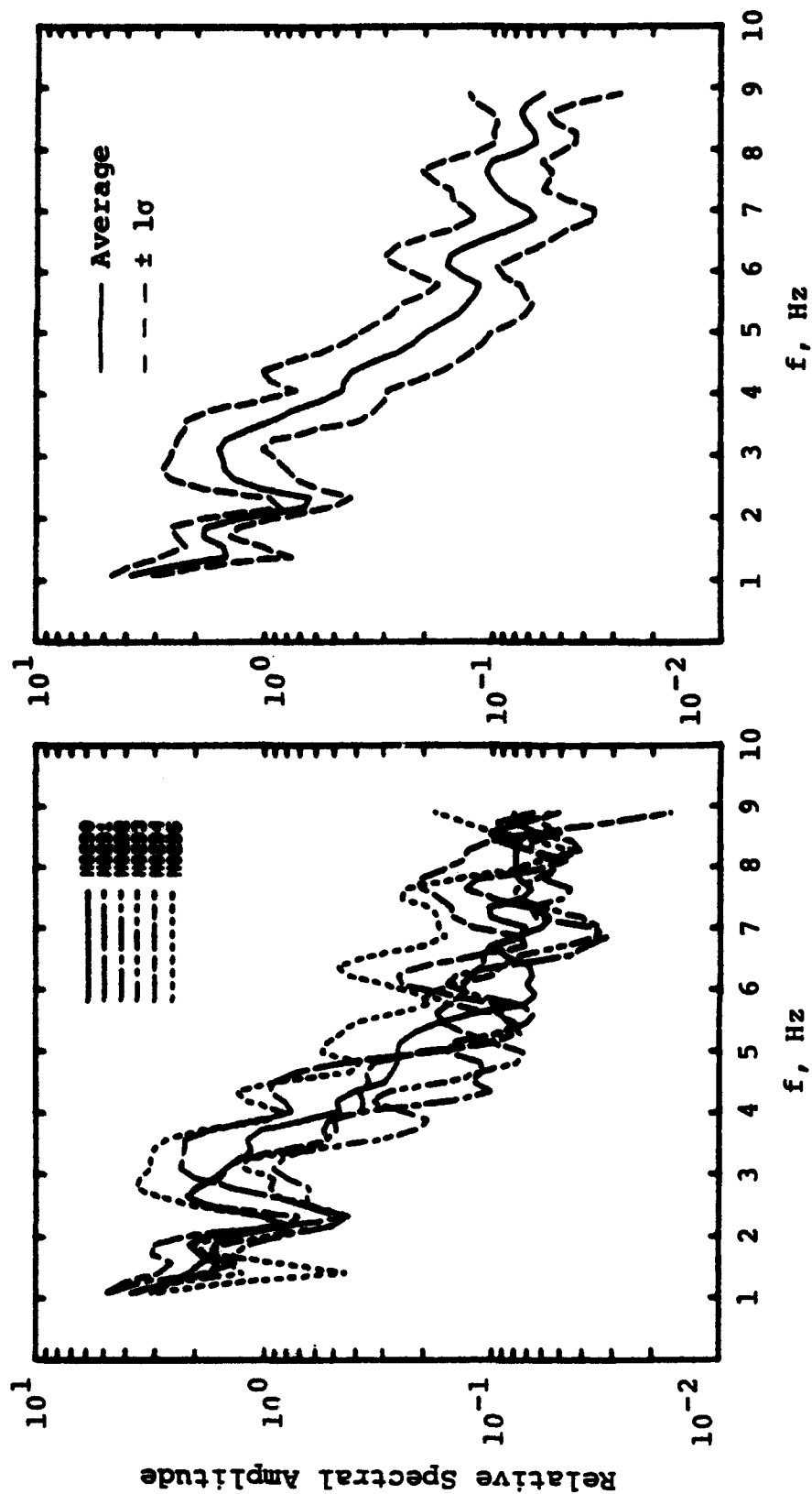


Figure 20. NOR SAR O2B single element (left) and subarray-averaged (right) P wave spectra for Event #10.

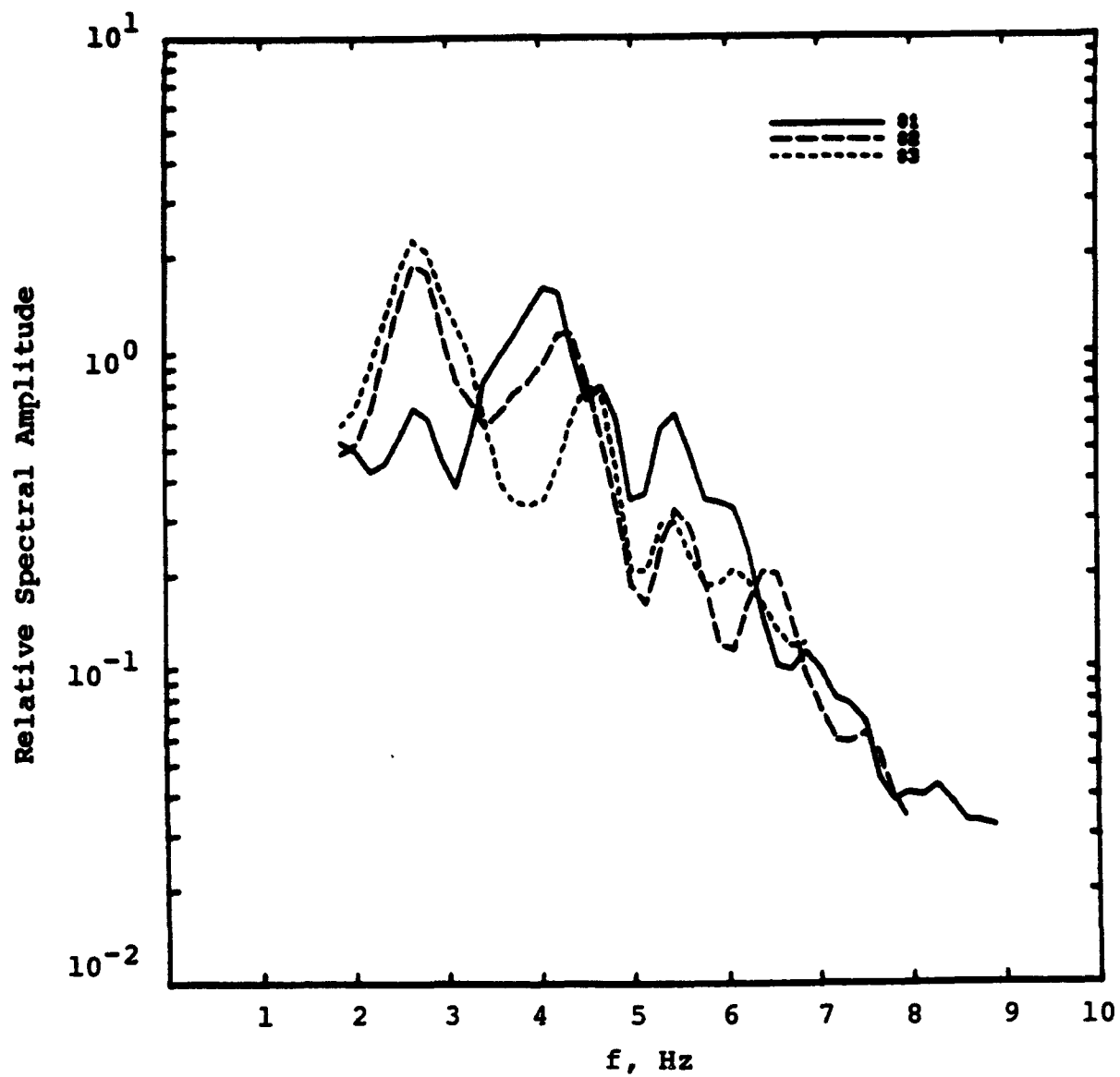


Figure 21. Comparison of NORSAR O2B subarray-averaged P wave spectra for Events #1-#3.

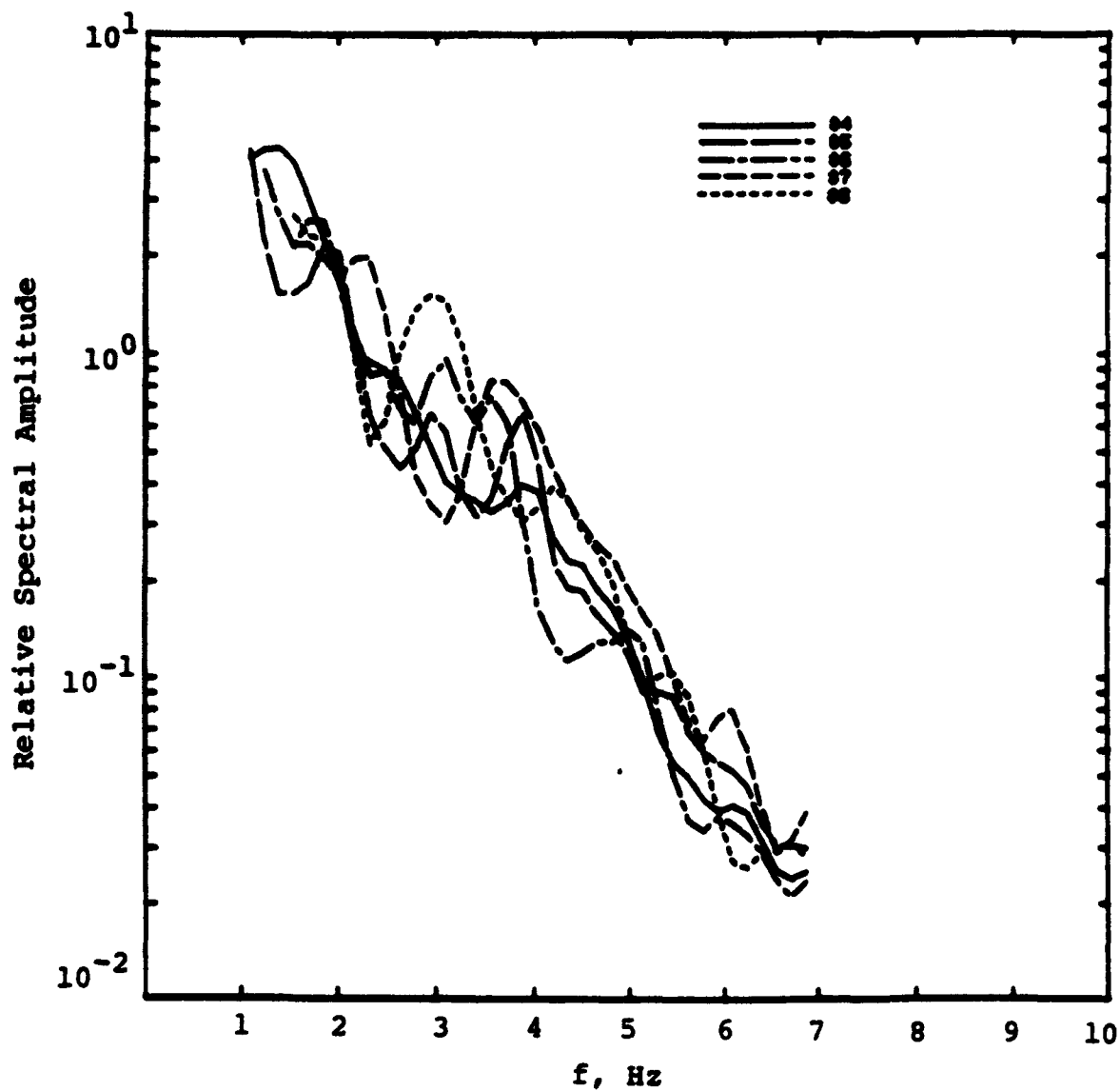


Figure 22. Comparison of NORSAR O2B subarray-averaged P wave spectra for Events #4-#8.

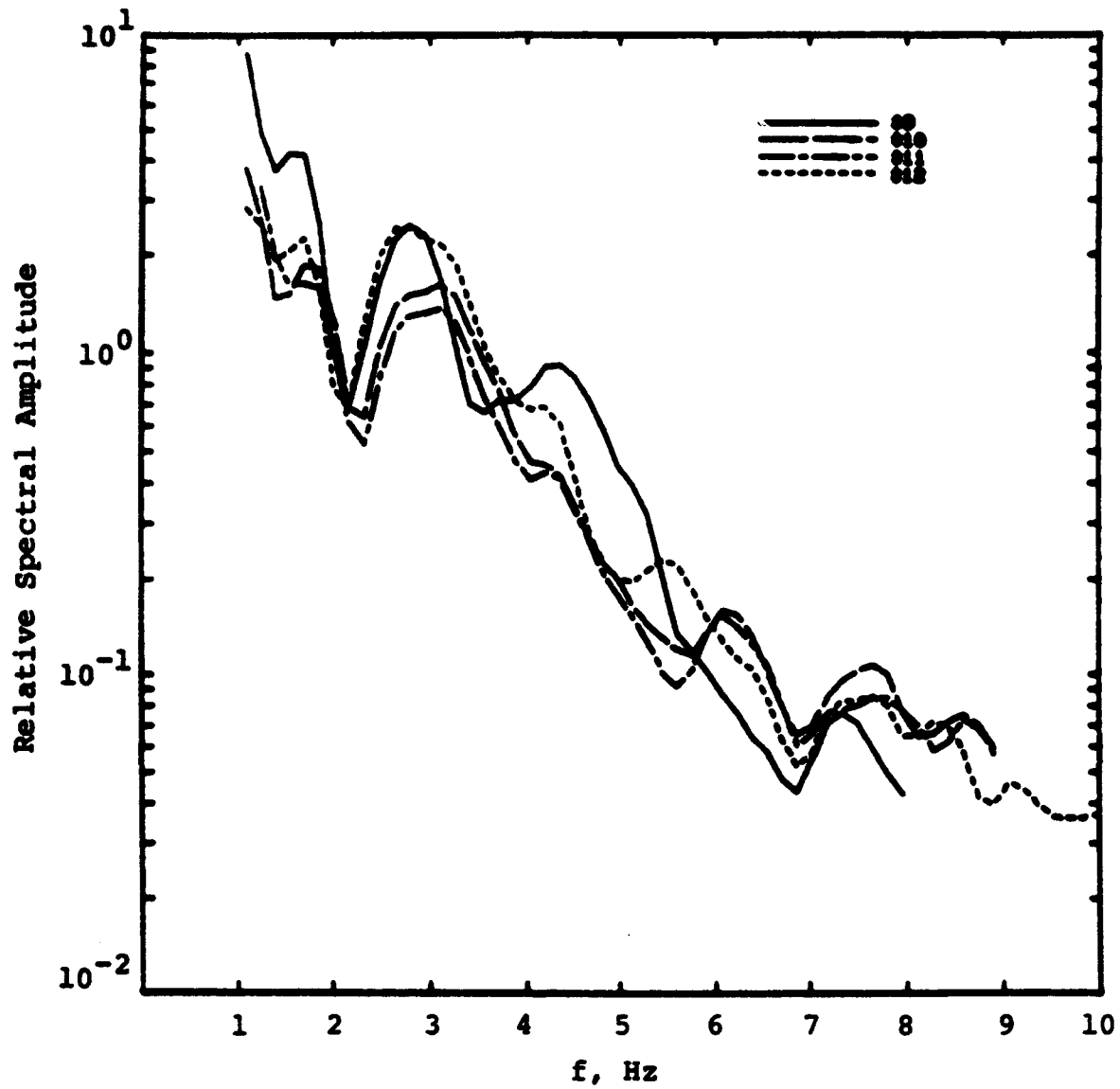


Figure 23. Comparison of NORSAR O2B subarray-averaged P wave spectra for Events #9-#12.

the same average amplitude level over the available passband. It can be seen that the spectral shapes within each group are quite consistent over the frequency band available for analysis. Thus, for example, the spectra for nuclear Events #10 and #11 in Figure 23 are essentially identical, as might be expected since they are of similar size and were detonated in the same cavity. More surprising is the close similarity of the P wave spectral shapes for the HE Events #4 - #8 in Figure 22, particularly considering the fact that they represent a range of source size and testing location. Figure 24 shows a comparison of the average spectra for each of the three groups of Figures 21-23, approximately normalized to the same low frequency level. It can be seen that the group consisting of the presumed chemical explosions #4 - #8 represents the lowest frequency source, while the group consisting of the presumed chemical explosions #1 - #3 appears to represent the broadest band source. Once again, as with the time domain characteristics, the average P wave spectra of the presumed chemical explosions in the two groups differ more from one another than either does from the average nuclear cavity P wave spectrum. This observation is illustrated more specifically in Figure 25 where the ratios of the average spectra for the two HE groups of events computed with respect to spectrum for cavity decoupled Event #9 are compared. This figure concisely summarizes the principal conclusion of the NORSAR analysis, which is that the variation of the characteristics of the recorded P waves from presumed chemical explosions envelopes the characteristics of the recorded P waves from nearby nuclear cavity explosions of comparable magnitude. Thus, this evidence suggests that teleseismic P wave data in the band from about 1 to 10 Hz is unlikely to provide a reliable basis for discriminating between these two source types.

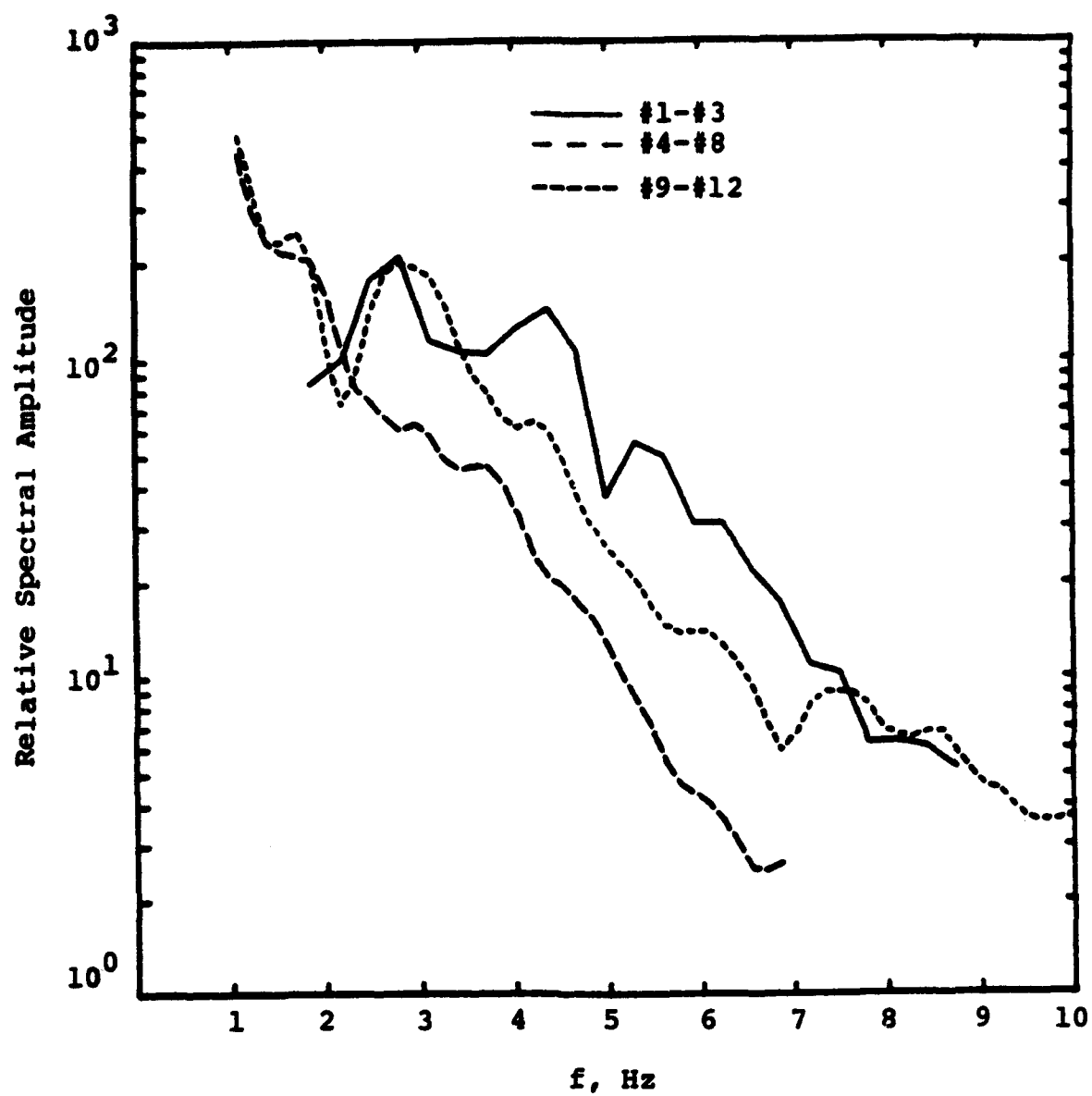


Figure 24. Comparison of NORSAR O2B P wave spectral average for Events #1-#3 with corresponding averages for Events #4-#8 and Events #9-#12.

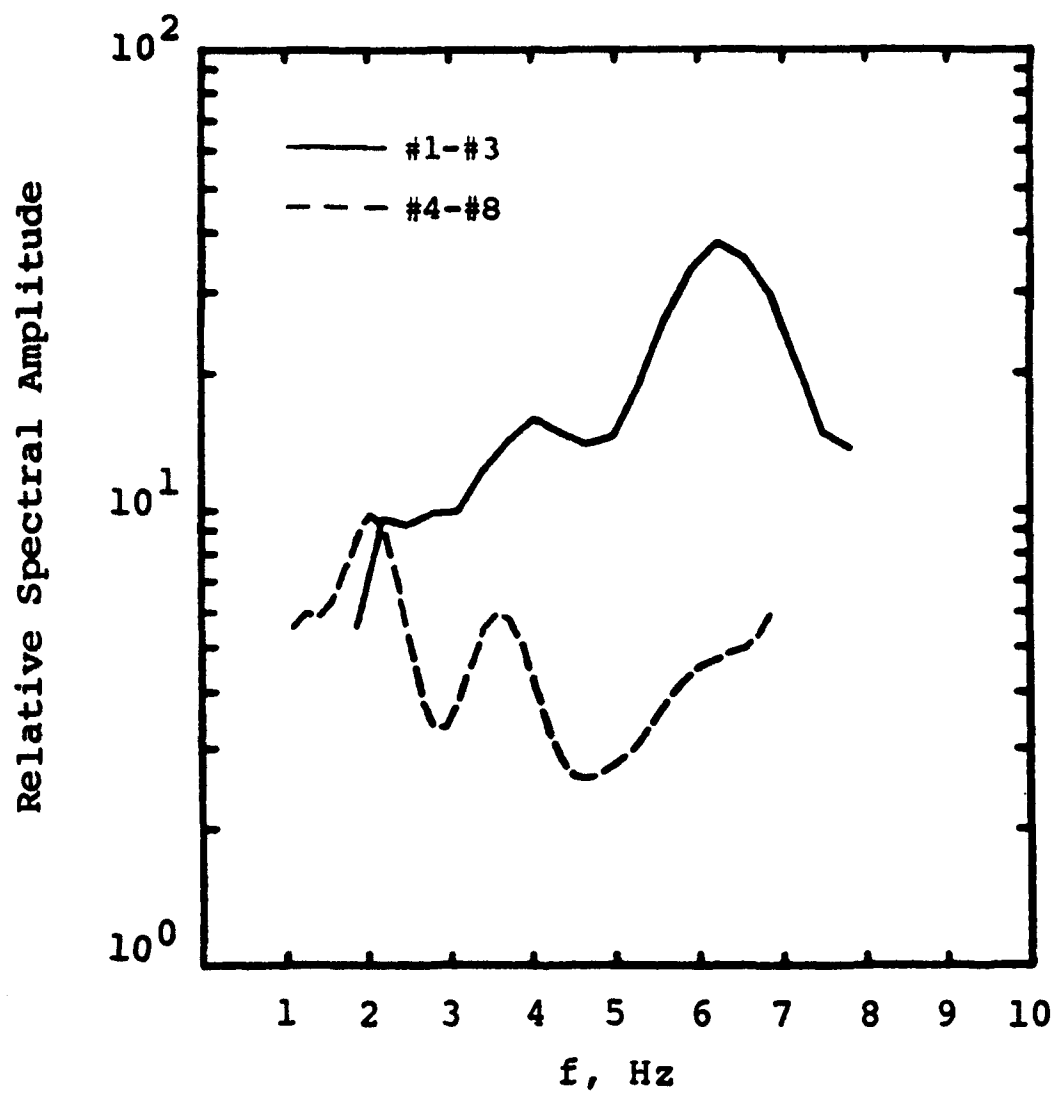


Figure 25. Comparison of ratios of average spectra for the two HE groups of events computed with respect to the spectrum for cavity decoupled nuclear Event #9.

4. Comparison of Broadband Near-Regional Seismic Recordings from Soviet CE and Cavity Decoupled Explosions in the Caspian Sea Region

As was noted in Section 3, we currently have knowledge of only two full scale nuclear decoupling experiments; namely, the U.S. test STERLING and the Soviet air-filled cavity test at Azgir. The Soviet cavity decoupling experiment was carried out on 3/29/76 when an 8 kt nuclear device was detonated at a depth of 987 m in a 38 m radius cavity in salt produced by a previous 64 kt tamped nuclear explosion conducted at that site on 12/22/71 (Adushkin *et al.*, 1992). Broadband seismic data were recorded from this decoupled test at near-regional distances ranging from about 1 to 113 km and these analog data were subsequently digitized at a rate of 200 samples/second, converted to ground motion amplitudes and installed as a database at the ARPA CSS (personal communication, I. Kitov, 1992). These data provide an important reference base for comparison with seismic data recorded in the same distance range from CE events in the Caspian Sea region. However, before comparisons can be made for the nominal, fully decoupled 1 kt evasion scenario, it is necessary to first normalize the observed data to account for the fact that the Azgir decoupling experiment was at a yield of 8 kt and was only partially decoupled. This has been accomplished using the approximate, theoretical scaling model described below.

Let $Z_1(t)$, $Z_2(t)$ denote the seismograms for a particular component of motion recorded at a fixed station from explosions at the same source location, with corresponding Fourier transforms $Z_1(\omega)$, $Z_2(\omega)$. Then, in operational form, the ground motion spectra can be written as

$$\begin{aligned} Z_1(\omega) &= S_1(\omega) T(\omega) \\ Z_2(\omega) &= S_2(\omega) T(\omega) \end{aligned} \quad (1)$$

where $S_1(\omega)$, $S_2(\omega)$ denote the seismic source functions corresponding to the two explosions and $T(\omega)$ is the propagation path transfer function which is common to both. It then follows that, to this degree of approximation

$$Z_2(\omega) = \frac{S_2(\omega)}{S_1(\omega)} Z_1(\omega) \quad (2)$$

$$Z_2(t) = \int_{-\infty}^{\infty} Z_1(\tau) S(t - \tau) d\tau \quad (3)$$

where $S(t)$ is the explosion source scaling operator. Thus, the expected ground motion time history for the second explosion can be determined from the observed ground motion from the first explosion if the spectral ratio of the two seismic source functions can be estimated. For the simplest, spherically symmetric model of the explosion source, the required source spectral ratio has the form (Mueller and Murphy, 1971)

$$\frac{S_2(\omega)}{S_1(\omega)} = \frac{p_2(\omega) \text{rel}_2}{p_1(\omega) \text{rel}_1} \frac{\omega_{o1}^2 + i \omega_{o1} \omega - \beta \omega^2}{\omega_{o2}^2 + i \omega_{o2} \omega - \beta \omega^2} \quad (4)$$

where rel_1 , rel_2 are the elastic radii of the two sources at which spherically symmetric pressures $p_1(\omega)$, $p_2(\omega)$ act and

$$\omega_{oi} = \frac{\alpha}{rel_i} \quad (5)$$

$$\beta = \frac{\lambda + 2\mu}{4\mu}$$

with α the P wave velocity and λ, μ the Lamé constants characteristic of the common source medium. Now for explosions at the same depth in a fixed medium, the elastic transition pressure should be constant then, assuming a step function approximation for the pressure profiles acting at the elastic radii, it follows that $p_2(\omega) = p_1(\omega)$ in (4) and the modulus of the source spectral ratio can be written simply as

$$|S(\omega)| = \left| \frac{S_2(\omega)}{S_1(\omega)} \right| = \frac{rel_2}{rel_1} \sqrt{\frac{(\omega_{o1}^2 - \beta\omega^2)^2 + \omega_{o1}^2\omega^2}{(\omega_{o2}^2 - \beta\omega^2)^2 + \omega_{o2}^2\omega^2}} \quad (6)$$

Thus, the low and high frequency asymptotic values of the source spectral ratio are given by

$$\begin{aligned} \lim_{\omega \rightarrow 0} |S(\omega)| &= \frac{rel_2 \omega_{o1}^2}{rel_1 \omega_{o2}^2} = \left(\frac{rel_2}{rel_1} \right)^3 \\ \lim_{\omega \rightarrow \infty} |S(\omega)| &= \frac{rel_2}{rel_1} \end{aligned} \quad (7)$$

or, since rel is proportional to the cube root of the yield W for explosions at a fixed depth in a given medium,

$$\lim_{\omega \rightarrow 0} |S(\omega)| = \frac{W_2}{W_1} \quad (8)$$

$$\lim_{\omega \rightarrow \infty} |S(\omega)| = \left(\frac{W_2}{W_1} \right)^{1/3}$$

This is the familiar cube root scaling model for the explosion seismic source function.

The time domain operator corresponding to Equation (6) for the case $\lambda = \mu$ has the form

$$S(t) = -\frac{\text{rel}_2}{\text{rel}_1} e^{-\frac{2}{3} \omega_{o2} t} \left[C_1 \cos \frac{2\sqrt{2}}{3} \omega_{o2} t + C_2 \sin \frac{2\sqrt{2}}{3} \omega_{o2} t \right] + \frac{\text{rel}_2}{\text{rel}_1} \delta(t) \quad (9)$$

where

$$C_1 = \frac{4}{3} (\omega_{o2} - \omega_{o1}) \quad (10)$$

$$C_2 = \frac{\sqrt{2}}{3} \omega_{o2} \left[1 + 2 \frac{\omega_{o1}}{\omega_{o2}} - 3 \left(\frac{\omega_{o1}}{\omega_{o2}} \right)^2 \right]$$

Then defining $S(t) = S_1(t) + (\text{rel}_2/\text{rel}_1) \delta(t)$ in (9), we can write

$$Z_2(t) = \int_{-\infty}^{\infty} Z_1(\tau) S_1(t - \tau) d\tau + \frac{\text{rel}_2}{\text{rel}_1} Z_1(t) \quad (11)$$

It follows that, given an observed seismogram from an explosion with known source characteristics, the seismogram to be expected at that same

station from an explosion with different source characteristics in the same region can be approximated using scaling relations of the form exemplified by Equations (9) - (11).

The simple scaling procedures described above have proven to work quite well in a number of different applications. For example, Figure 26 shows the results of scaling observed STERLING data from near-regional station 10S at a range of 16 km to the source conditions of SALMON using the source parameters inferred by Murphy (1969) for these two explosions. It can be seen that, despite the simplicity of the source approximations, the agreement between the scaled STERLING and observed SALMON seismic data at this station is quite remarkable. This would seem to confirm the validity of the procedure as applied to co-located events in the same medium. A remaining question concerns the applicability of SALMON/STERLING seismic source scaling and decoupling relations to explosions in the Azgir salt domes. Although additional work is needed to fully assess the consistency of the seismic source coupling in these different salt environments, some recently acquired Soviet free-field data from a tamped explosion at Azgir suggests that they might be quite similar. These new free-field data were recorded from the 1.1 kt tamped nuclear explosion which was conducted at a depth of 161 m at Azgir on 4/22/66. For this test, vertical component particle velocity waveforms were measured above the detonation point at ranges extending from 63 to 161 m in a satellite hole offset from the emplacement hole by about 10 m (personal communication, I. Kitov, 1993). Using simple cube-root scaling as a first approximation, the recording made at a range of 84 m above shot depth corresponds to a range of 142 m at the 5.3 kt yield of SALMON. The cube-root scaled version of this recording is shown in Figure 27 where it is compared with the SALMON shot depth recording at a range of 166 m. It can be seen that the arrival times, waveshapes and amplitude levels (preliminary for Azgir) are remarkably similar for these two recordings, which suggests that the seismic source coupling characteristics of Azgir salt may not be very different from those of SALMON salt. Additional data will have to be analyzed in order to definitively test this hypothesis. However, these preliminary data suggest

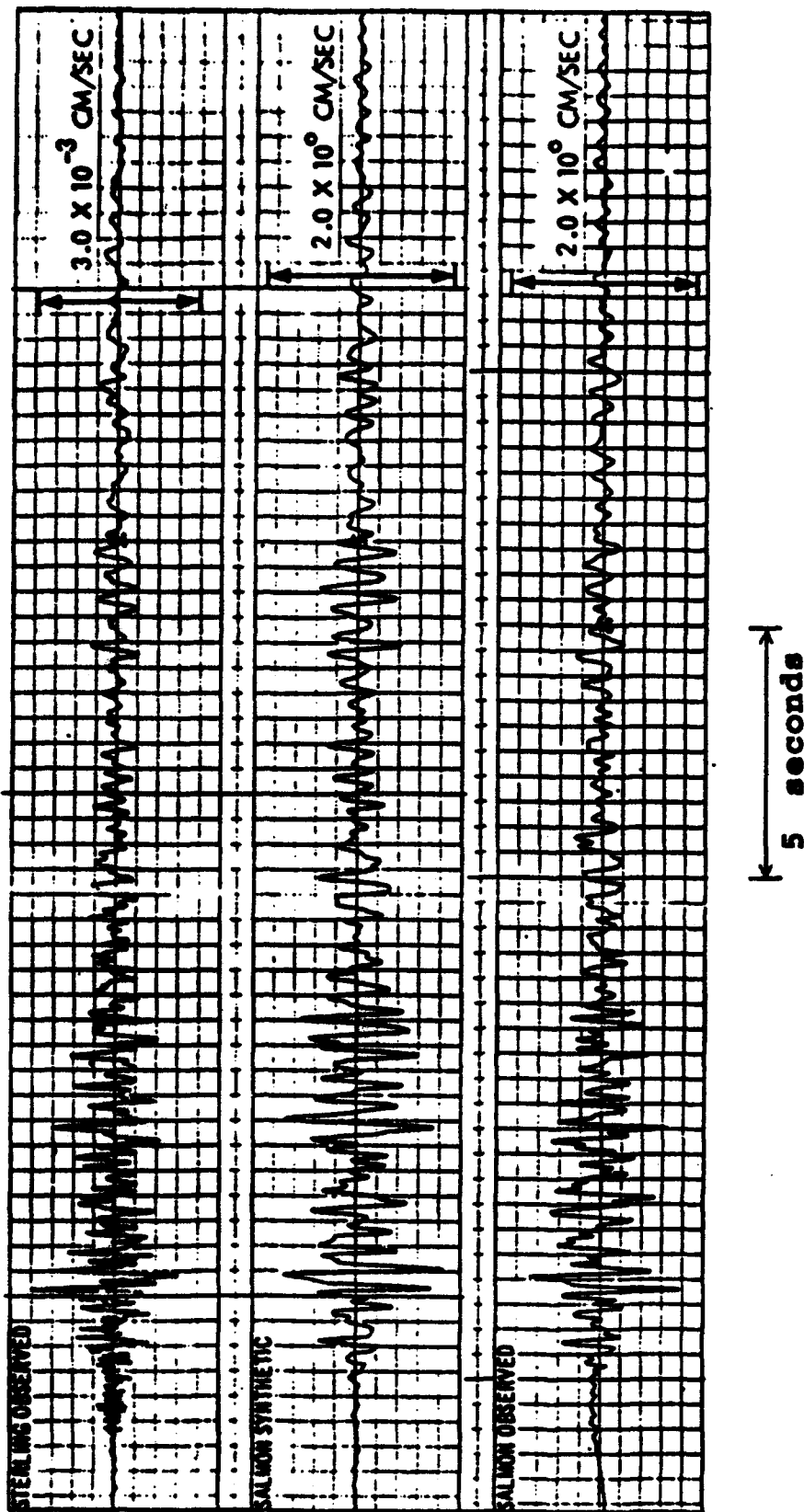


Figure 26. Comparison of observed SALMON and scaled STERLING (SALMON synthetic) radial component seismograms for station 10S.

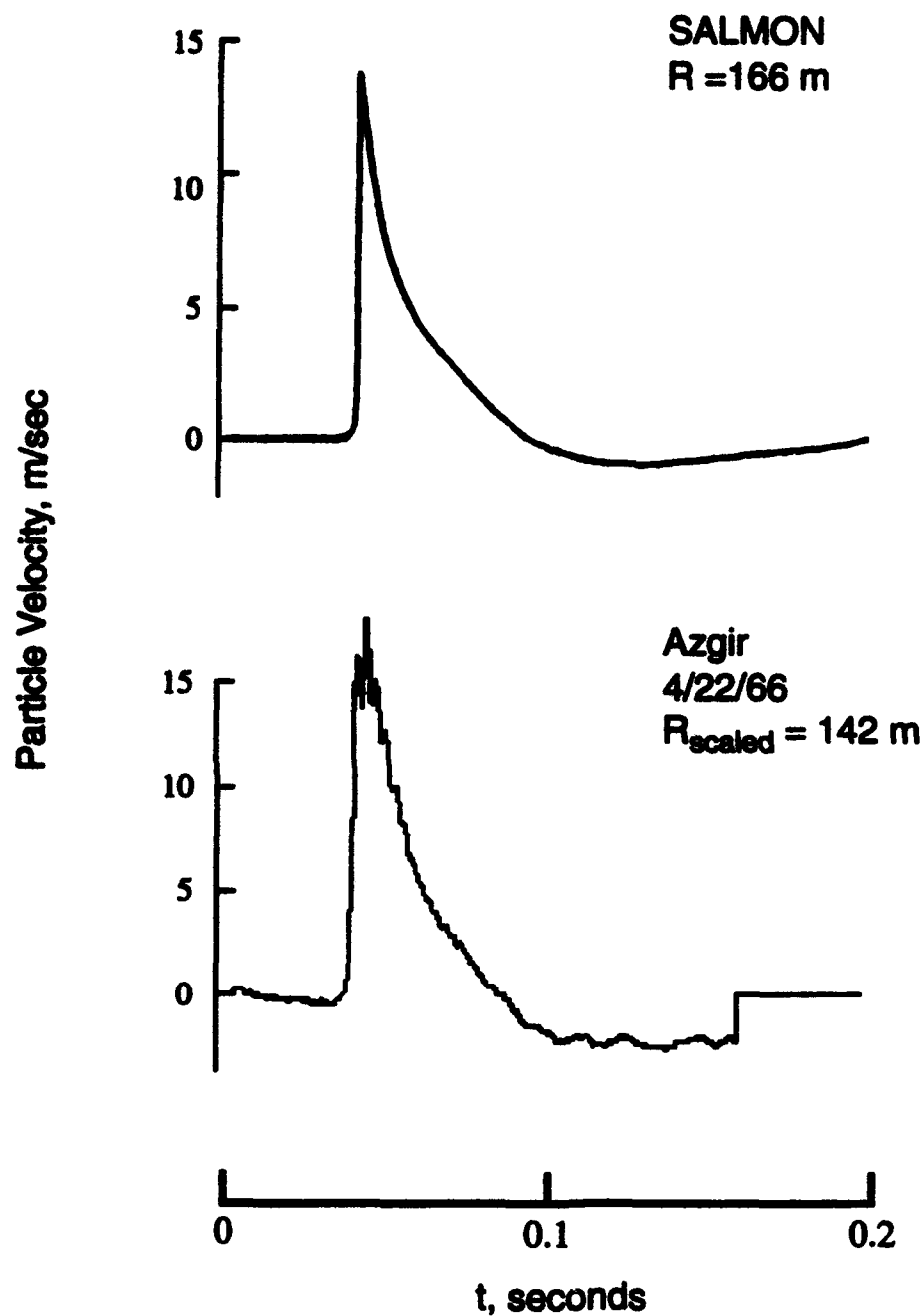


Figure 27. Comparison of observed SALMON free-field particle velocity recording at a range of 166 m with the cube-root scaled Azgir 4/22/66 free-field particle velocity recording at a scaled range (at 5.3 kt) of 142 m.

that the SALMON/STERLING source scaling procedures, illustrated by the results shown in Figure 26, should provide a reasonable first approximation for application to Azgir explosion data.

The vertical component displacement waveforms recorded from the Azgir cavity decoupling test of 3/29/76 in the near-regional distance range extending from about 18 to 113 km are shown in Figure 28. It is evident that these data are quite complex and variable as a function of distance. Thus, for example, it can be seen that while the first arrival at 25.5 km is impulsive and simple, that at the nearby 23.0 km station is much more emergent and complex. Similar comments apply to the observations at distances greater than 40 km, which show no obvious explosion-like characteristics of the kind which frequently distinguish teleseismic P waves recorded from underground explosion sources. This observed high degree of variability is typical of broadband, near-regional recordings from earthquakes and explosions and contributes to the difficulty of defining reliable discriminants for application in this distance range.

Now, before the data of Figure 28 can be scaled to that expected for the 1 kt fully decoupled scenario, it is necessary to first define an approximate seismic source model for this 8 kt partially decoupled explosion. Detailed, nonlinear finite difference simulations of this source are currently underway but, for the present application, we will employ the simplest analytic approximation corresponding to a step in pressure acting at the elastic radius. Preliminary modeling of the near-field P wave spectra for this test suggests an equivalent elastic radius of about 50 m, a value which is significantly larger than the initial cavity radius of 38 m. This is not surprising, since a cavity with a radius of more than 45 m would be required to match STERLING conditions for 8 kt at this depth. It follows that cube-root scaling to the comparable conditions of 1 kt in a 19 m radius cavity at the depth of the Azgir cavity should give an elastic radius of about 25 m. The source spectral ratio corresponding to Equation (6) for this 8 kt to 1 kt scaling operator is shown as a dashed line in Figure 29, where it can be seen that the low frequency level is equal to 0.125 (i.e., $(25/50)^3$) and the

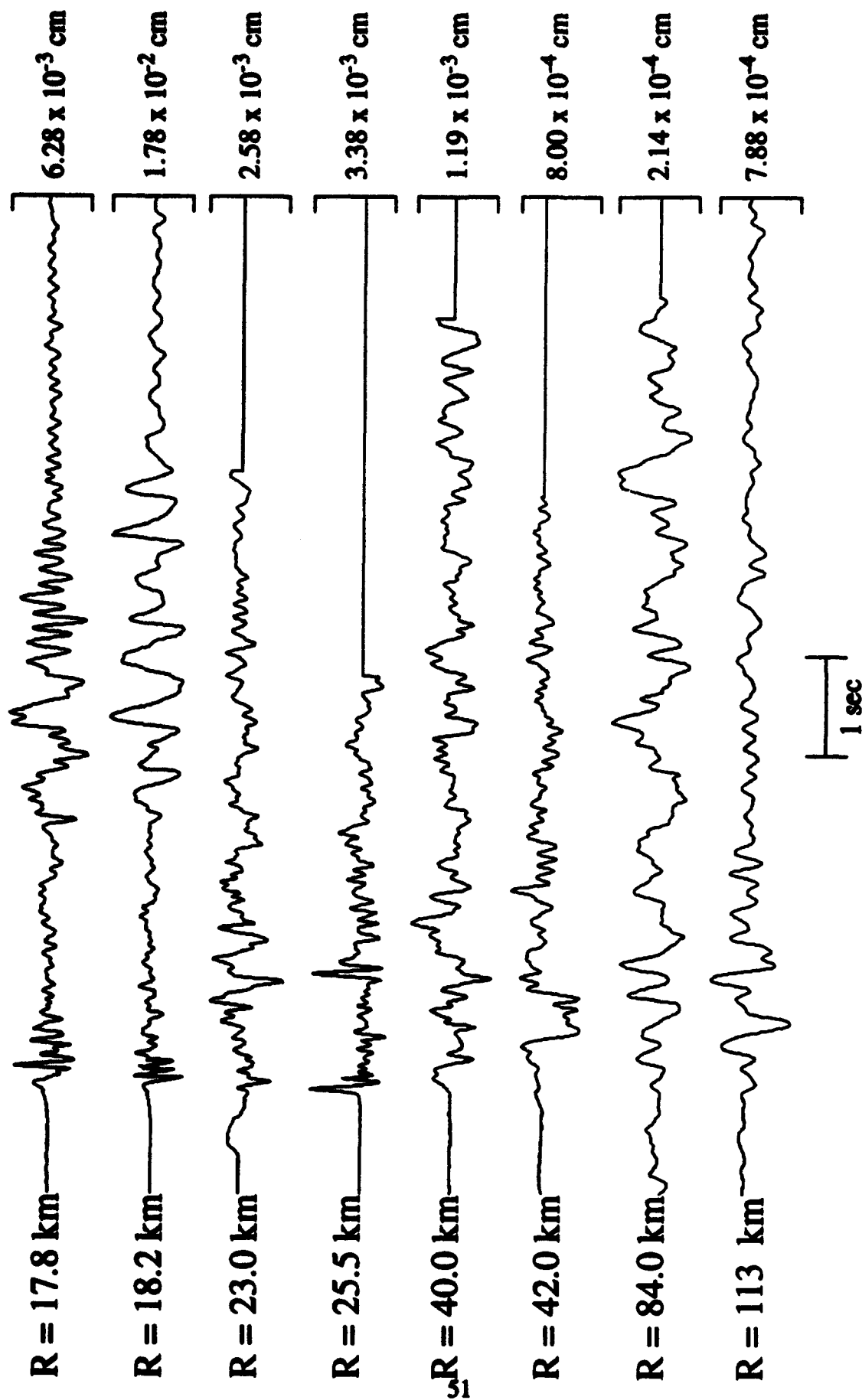


Figure 28. Vertical component ground motions recorded from the 8 kt Azgir cavity decoupling test of 3/29/76.

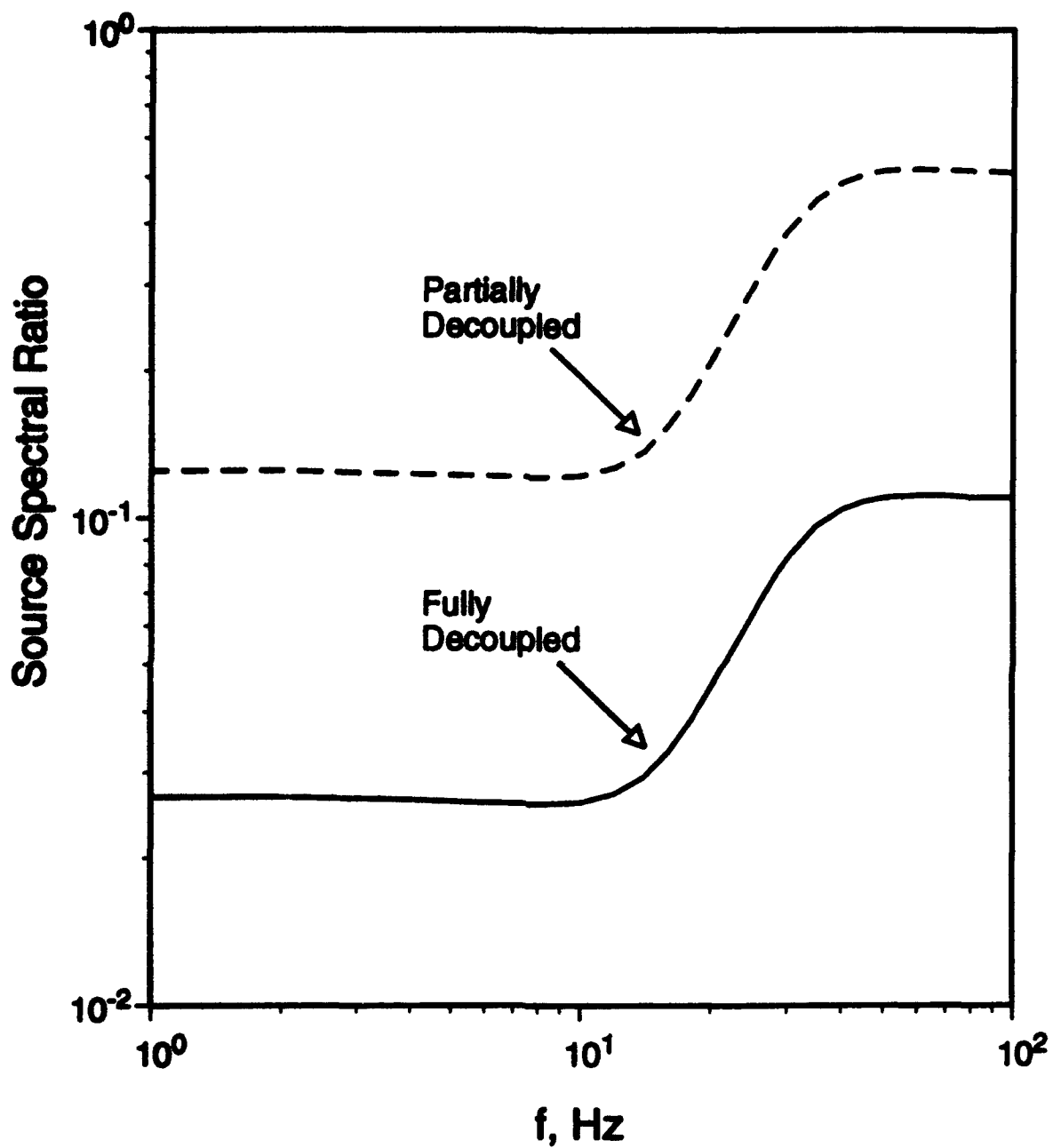


Figure 29. Comparison of approximate source scaling operators for partially (dashed) and fully (solid) decoupled 1 kt explosions, estimated relative to the partially decoupled 8 kt Azgir cavity explosion of 3/29/76.

high frequency level is equal to 0.5 (i.e., 25/50) in accord with the asymptotic relations given by Equations (8). Now the observed decoupling factor for the 3/29/76 Azgir test was about a factor of 15 (Adushkin et al., 1992), as opposed to the observed STERLING nominal "full" decoupling factor of 70. Therefore, in order to approximately scale to STERLING decoupling conditions for 1 kt at Azgir, the source scaling operator represented by the dashed line in Figure 29 has been multiplied by the ratio 15/70 to obtain the final source scaling operator shown as the solid line in Figure 29. This is the operator which has been used to scale the near-regional data observed from the 8 kt partially decoupled Azgir test to approximate the ground motions which would be expected from a 1 kt fully decoupled explosion at that same source location. Note that for frequencies less than about 15 Hz, this operator is nearly constant, independent of frequency, at a level given by the low frequency asymptotic value of Equation (8). It follows that since the observed 8 kt decoupled Azgir data of Figure 28 are dominated by components having frequencies less than about 10 Hz, the expected effect of scaling to the 1 kt fully decoupled scenario is to reduce the amplitude level by about a factor of 40 without significantly modifying the time dependent character of the signals. This expectation is confirmed in Figure 30 which shows the approximations to the 1 kt fully decoupled ground motions obtained by applying the solid line source scaling operator of Figure 29 to the observed Azgir waveforms of Figure 28. Comparing Figures 30 and 28, it can be seen that the relative spectral composition of the signals is unchanged by scaling in this case, in contrast to the pronounced change for the SALMON/STERLING scaling results shown previously in Figure 26. The inferred peak vertical component displacement amplitudes from Figure 30 are plotted versus range in Figure 31 where it can be seen that they decrease with distance at an average rate about equal to that reported by Adushkin *et al.* (1992) for tamped explosions at Azgir.

Unfortunately, no data from CE events have been recorded at the stations used to record the Azgir nuclear decoupling test. However, numerous mine blasts have been recorded in the same near-regional distance range at IRIS station KIV which is located west of the Caspian Sea at

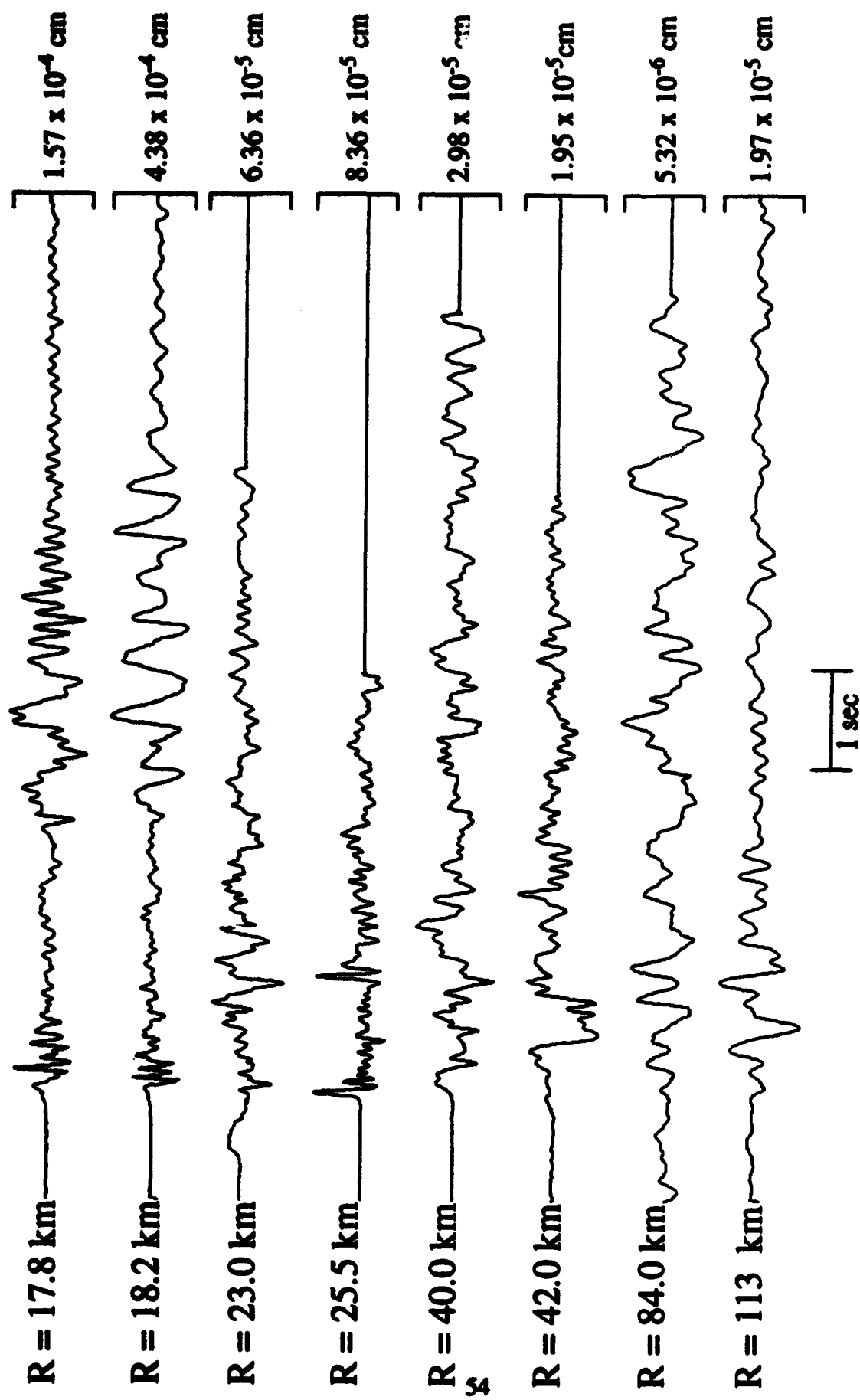


Figure 30. Theoretically scaled vertical component ground motions corresponding to a 1 kt fully decoupled explosion at the source location of the 8 kt Azgir decoupling test of 3/29/76.

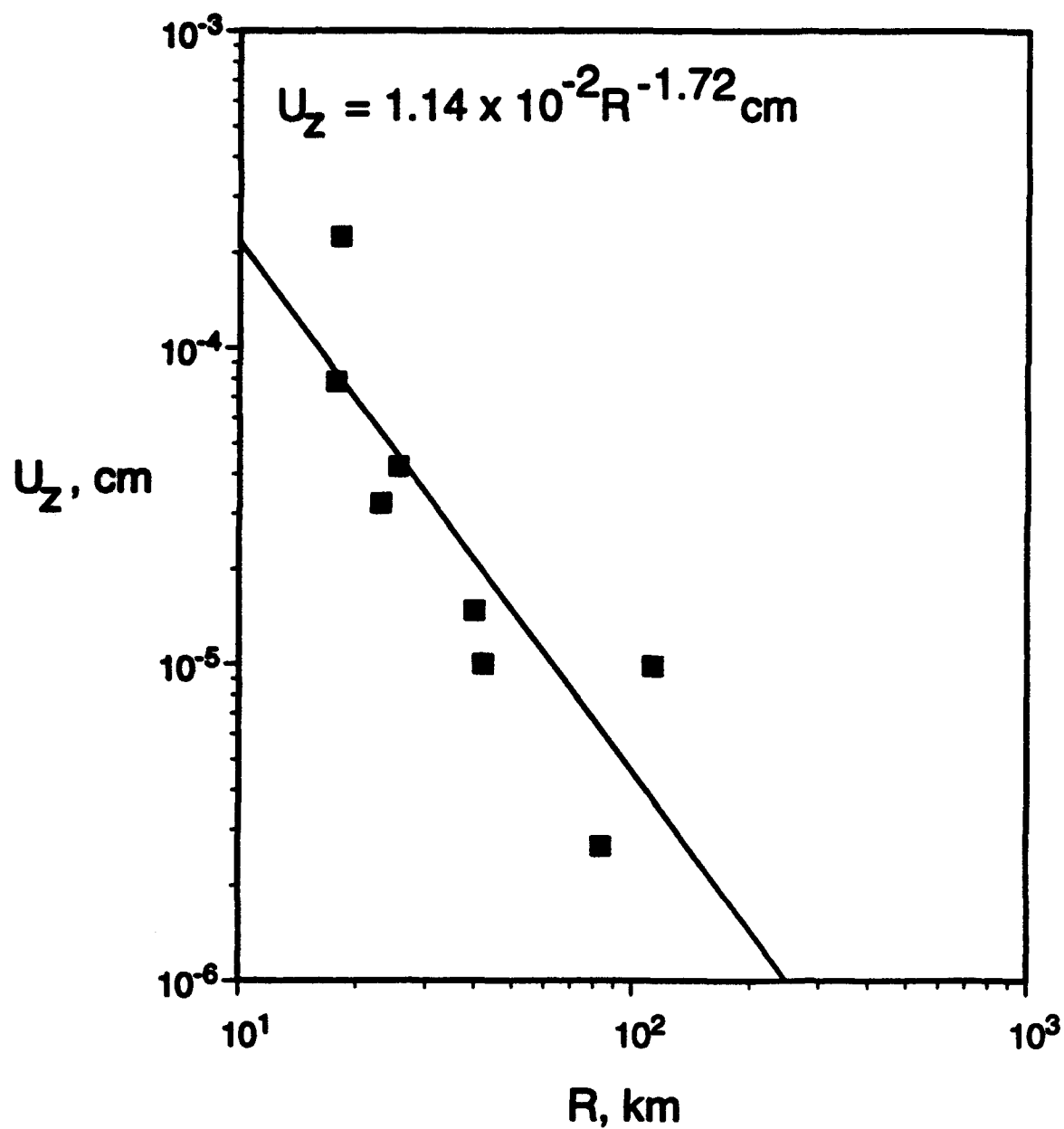


Figure 31. Estimated peak vertical displacements as a function of distance for a fully decoupled 1 kt cavity explosion at Azgir.

Kislovodsk, approximately 600 km southeast of Azgir. The location of station KIV with respect to Azgir is shown in Figure 32, which also shows in expanded scale the locations of two mines near KIV, as well as the locations of five satellite stations surrounding KIV which have recorded seismic data from blasts at these two mines (Rivière-Barbier, 1993). These stations recorded data at an extended sampling rate of 125 samples/second from two well-documented explosions at the Tyrnyauz mine and one at the Zhako-Krasnogorskaya mine which provide a broadband, near-regional seismic data base comparable to the Azgir nuclear decoupling data recorded in the same distance range. According to Rivière-Barbier (1993), the two well-documented Tyrnyauz mine blasts were conducted about one minute apart on 4/12/92. Both were ripple-fired explosions detonated in multiple boreholes extending to a depth of 15.6 m below the surface of the open pit mine. The first, denoted 4/12/92(1), a total yield of 27 tons of CE, while the second, denoted 4/12/92(2), had a total yield of 70 tons CE. The documented blast at the Zhako-Krasnogorskaya mine occurred on 5/8/92 and was also a ripple-fired, multiple borehole explosion at the surface of this gypsum pit mine, having a total yield of 11.9 tons CE.

Before proceeding to waveform comparisons, it is appropriate to examine the amplitude levels of the ground motions produced by these mine blasts as they relate to those expected in the same distance range from the nominal 1 kt fully decoupled nuclear explosion at Azgir. The peak vertical displacements observed at the KIV station array from the three well-documented mine blasts are displayed as a function of range in Figure 33. On these figures, the dashed lines represent the average 1 kt fully decoupled amplitude-distance relation from Figure 31 and the solid lines represent the attenuation relations of the same slope which provide best fits to the observed ground motion amplitudes for these three mine blasts. The vertical arrows with annotated values indicate the average multiplicative factors separating these two lines in each case. Now, since a 1 kt fully decoupled explosion is expected to produce low frequency seismic motions with amplitudes comparable to those expected from a 14 ton (i.e., 1000 tons/70) fully tamped nuclear explosion at the same source location, it might be

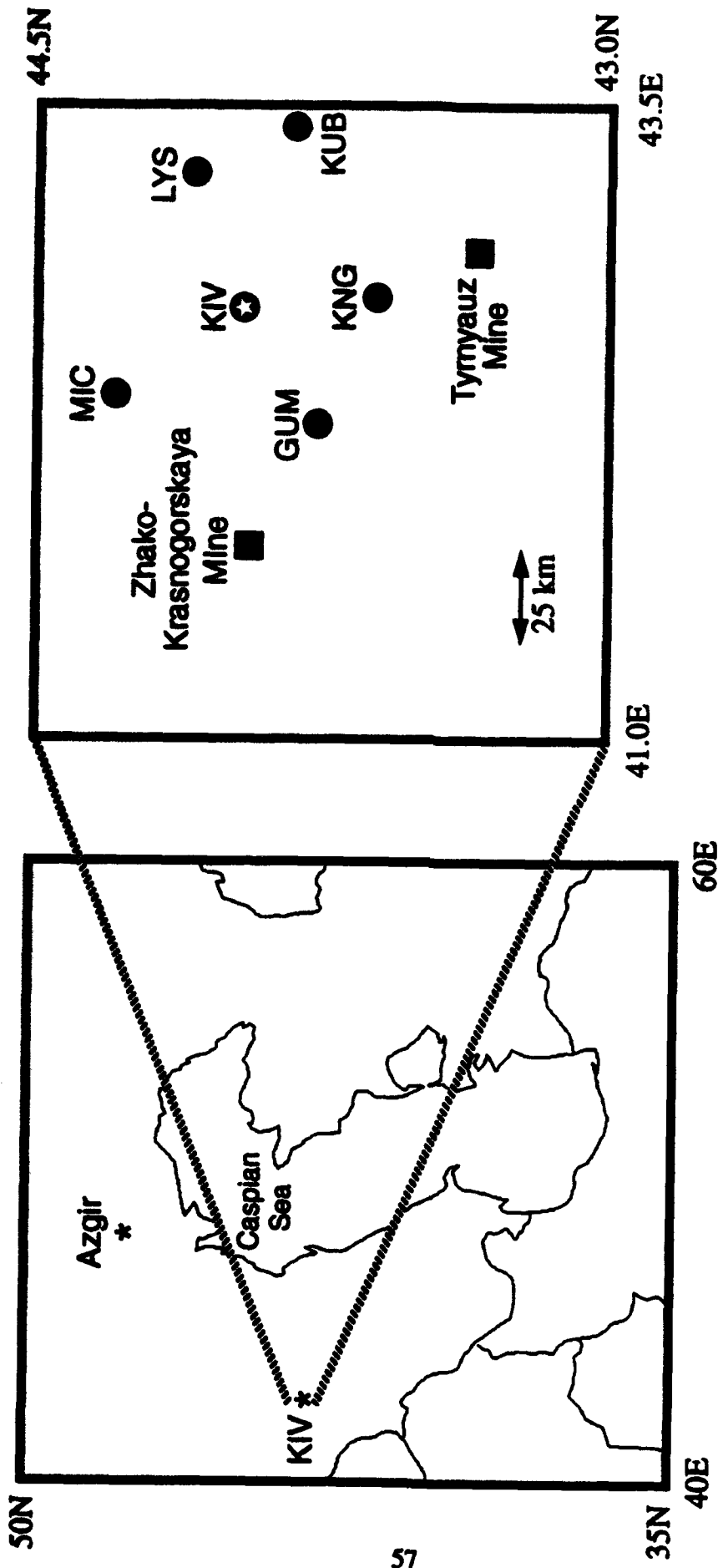


Figure 32. Map location of IRIS station KIV with respect to the Azgir test site. The expanded display at the right shows the locations of selected mines and broadband recording stations around KIV.

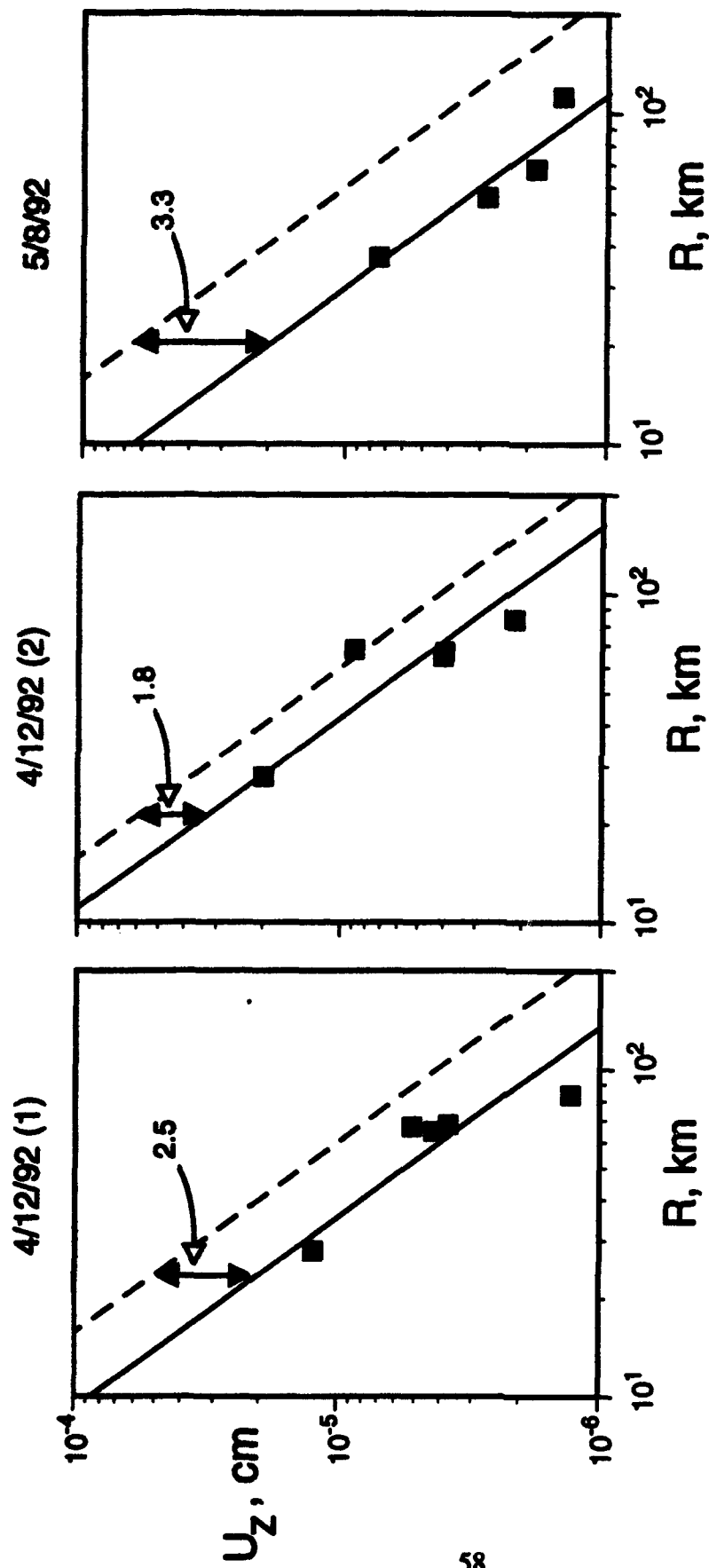


Figure 33. Comparison of peak vertical displacement levels observed from three well-documented Caspian mine blasts (solid) with the corresponding displacement levels expected from a fully decoupled 1 kt nuclear explosion at Azgir (dashed).

expected that the displacement amplitudes from the 1 kt decoupled test would be comparable to those observed from the 5/8/92 11.9 ton CE test and significantly lower than those observed from the 4/12/92(1) 27 ton and 4/12/92(2) 70 ton CE tests. However, it can be seen from Figure 33 that, in fact, the average 1 kt nuclear decoupled amplitude levels represented by the dashed lines lie well above the observed CE amplitude levels in all three cases. These observations are consistent with the theoretical simulation results reported by Barker *et al.* (1992) which indicate that the seismic coupling efficiencies of ripple-fired, excavation CE blasts are significantly lower than those to be expected from contained underground nuclear explosions of comparable yield. The comparisons of Figure 33 suggest that, on average, a CE mine blast with a yield of about 75 tons at these mines would be required to produce the same low frequency ground motion amplitudes as a 1 kt fully decoupled or 14 ton tamped underground nuclear explosion. That is, the low frequency seismic coupling efficiency of these CE mine blasts is on the order of a factor of five lower than that expected from a tamped nuclear explosion of comparable yield. Of course, significant deviations from this average coupling difference can be expected in individual cases due to variations in blasting practice.

Selected vertical component ground motions observed from the two 4/12/92 Tyrnyauz mine blasts are shown in Figure 34 where they are compared with scaled Azgir ground motions recorded from the 3/29/76 cavity decoupled nuclear test in the same near-regional distance range. It can be seen that there are no obvious differences between these recorded ground motions which would permit an analyst to visually discriminate between the two source types. Of course, this conclusion is contingent on the unstated assumption that there are no major differences in regional phase propagation characteristics between the Azgir and KIV sites which might be obscuring source related differences in the recorded signals. This assumption will have to be tested more carefully in the next phase of this investigation. In any case, the preliminary comparisons shown in Figure 34 suggest that it will not be a trivial matter to discriminate between CE and cavity decoupled nuclear explosions using broadband, near-regional seismic

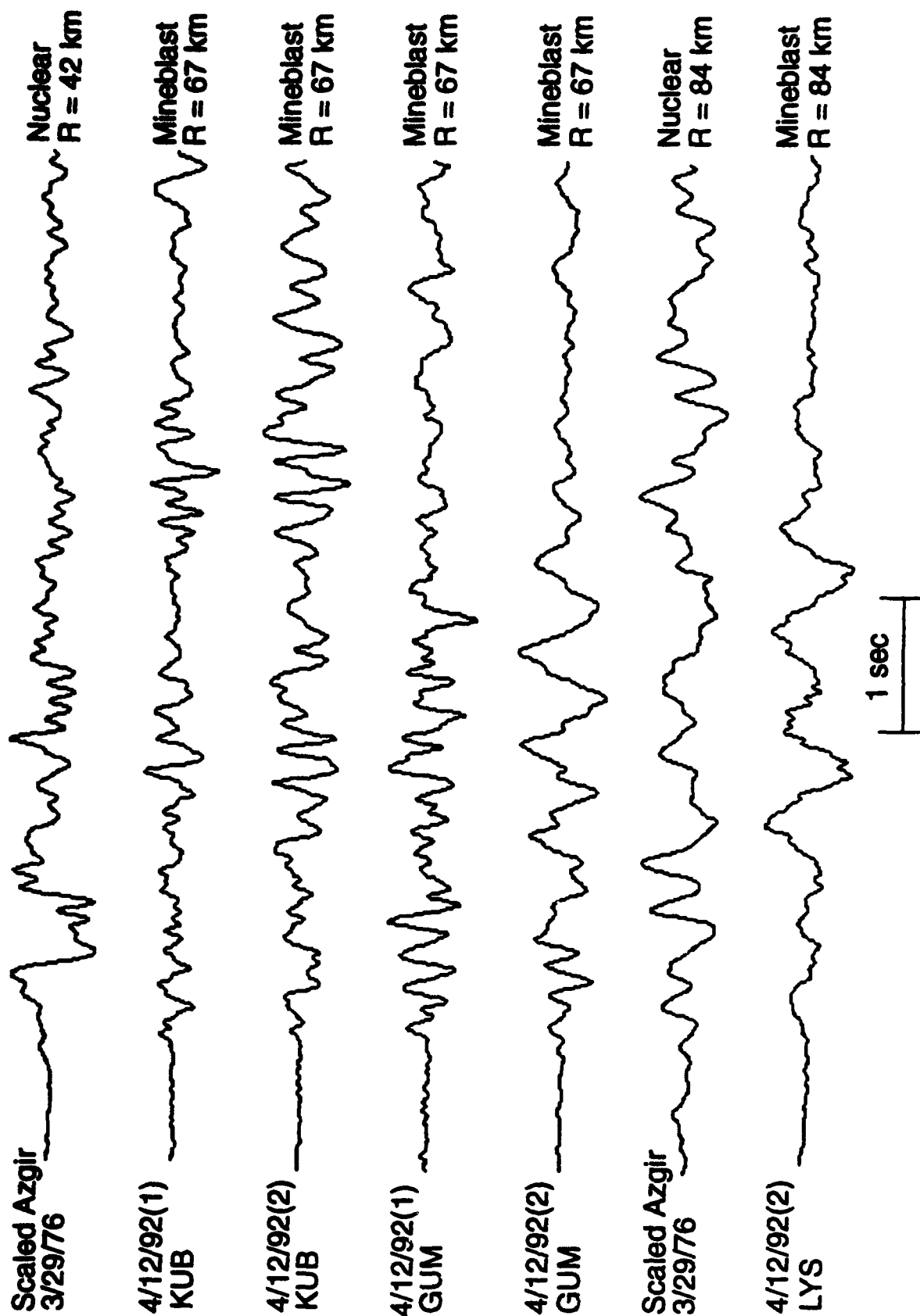


Figure 34. Comparison of scaled Azgir 1 kt fully decoupled ground motion estimates with the ground motions recorded in the same near-regional distance range from CE blasts at the Tyrmyauz mine.

data. Additional research will be required to determine whether more detailed and sophisticated comparisons of the data will provide a reliable seismic procedure for identifying small, cavity decoupled nuclear explosions in a background consisting of large numbers of CE events of comparable magnitude.

5. Summary and Conclusions

5.1 Summary

Successful seismic monitoring of any eventual Comprehensive Test Ban Treaty will require the development of a reliable capability to identify seismic signals from small, cavity decoupled nuclear explosions from among the numerous signals to be expected from earthquakes and CE events of comparable magnitude. The preliminary investigations summarized in this report have centered on a variety of comparative analyses of observed and simulated seismic data corresponding to decoupled nuclear explosions and different types of CE events. In particular, data recorded from cavity decoupled nuclear tests conducted in both the U.S. and former Soviet Union have been used as points of reference for evaluating potential seismic discriminants which might be used to differentiate such sources from CE events occurring in the same source regions.

Near-regional seismic data recorded from the U.S. nuclear cavity decoupling experiment STERLING and the nearby tamped CE test STERLING HE were compared in Section 2, where the time and frequency domain characteristics of the signals were examined in detail. It was found that, although the relative spectral compositions of the P and S waves observed from these two sources appear to be roughly comparable, the S/P spectral ratios are significantly higher for STERLING HE than for STERLING over a broad frequency band extending from at least 1 to 10 Hz. Preliminary evaluation of possible causes of this difference seems to rule out differences in charge geometry, but differences in locations of the two sources within the Tatum salt dome structure remains as a possible explanation which needs to be tested more rigorously in future studies.

Short-period P wave data recorded at NORSAR from Soviet nuclear tests conducted in salt cavities at Azgir and from nearby CE events were

compared in Section 3 where the array data were processed to obtain average P wave spectra for each selected event. The results of this signal processing analysis were then used to demonstrate that the variation of the spectral characteristics of the recorded P waves from the different types of CE events envelopes the spectral characteristics of the recorded P waves from nearby nuclear cavity explosions of comparable magnitude. This evidence was interpreted as an indication that teleseismic P wave data in the band from about 1 to 10 Hz are unlikely to provide a reliable basis for discriminating between these two source types.

Finally, in Section 4, broadband seismic data recorded at near-regional Soviet stations from an Azgir nuclear cavity decoupling test were theoretically scaled to the 1 kt fully decoupled level and compared with data recorded at the nearby IRIS station KIV from well-documented CE events. Using the results of these comparisons, it was shown that the ground motion amplitude levels corresponding to the 1 kt fully decoupled nuclear test are, on average, a factor of five larger than those observed from near-surface mine blasts of comparable energy release, in agreement with the results of previous finite difference simulations of the relative seismic coupling efficiency of these two source types. Moreover, the broadband, near-regional ground motion time history data recorded from these events were shown to be highly complex and variable and not obviously indicative of source type. These preliminary findings were interpreted as an indication that additional, innovative research will be required to define a reliable seismic procedure for identifying small cavity decoupled nuclear explosions using broadband, regional data.

5.2 Conclusions

The research summarized above supports the following preliminary conclusions regarding the seismic identification of small, cavity decoupled nuclear explosions.

- (1) The STERLING HE test produced seismic signals with amplitude levels which are about twice as large as those expected from a tamped nuclear explosion of comparable energy release. It follows that a tamped CE test with a yield of about 7 tons would be expected to produce ground motion amplitudes equal to those expected from a 1 kt fully decoupled nuclear cavity test.
- (2) The S to P wave spectral ratios for STERLING HE are significantly higher than those for STERLING over a broad frequency band extending from at least 1 to 10 Hz. This appears to be unrelated to differences in charge geometry between the two tests, but may correlate, at least partially, with differences in source location within the Tatum salt dome structure.
- (3) The variations of the spectral characteristics of the short-period P waves recorded at NORSAR from CE events near Azgir envelope the characteristics of the corresponding P wave spectra for nuclear cavity explosions of comparable magnitude at the Azgir test site. This evidence suggests that teleseismic P wave data in the band from about 1 to 10 Hz are unlikely to provide a reliable basis for discriminating between these two source types.
- (4) Observed seismic data from nuclear tests can be theoretically scaled to other hypothetical source conditions with reasonable accuracy using simple, analytic approximations to the nuclear seismic source functions. In particular, experience with SALMON/STERLING indicates that the procedure is applicable to the simulation of ground motions expected from low yield cavity decoupled explosions.
- (5) Preliminary comparisons of free-field ground motion data recorded from a tamped nuclear explosion in salt at Azgir with corresponding SALMON free-field data suggest that the seismic source coupling is quite similar for these two salt domes.

- (6) Comparisons of the seismic amplitude levels corresponding to a 1 kt fully decoupled nuclear cavity test at Azgir with the amplitude levels observed from well-documented surface mine blasts at IRIS station KIV indicate that the seismic coupling efficiency of these ripple-fired CE events is about a factor of 5 lower than that expected from a tamped nuclear explosion of comparable energy release. It follows that ripple-fired mine blasts with explosive yields of about 70 tons would be expected to produce seismic signals with amplitude levels equal to those to be anticipated from a 1 kt fully decoupled nuclear cavity test.
- (7) Comparisons of near-regional ground motion time histories corresponding to a 1 kt fully decoupled nuclear cavity test at Azgir with ground motion data recorded in the same distance range from ripple-fired mine blasts at station KIV, reveal no obvious differences which would permit an analyst to visually distinguish between the signals from these two source types. It is concluded that more detailed and sophisticated comparisons of such data will be required before it can be determined whether a reliable seismic procedure can be defined for identifying small, cavity decoupled nuclear explosions in a background consisting of signals from numerous CE events of about the same magnitude.

REFERENCES

- Adushkin, V. V., I. O. Kitov and D. D. Sultanov (1992), "Experimental Results of USSR Nuclear Explosion Decoupling Measurements," Paper presented at the 14th Annual PL/DARPA Seismic Research Symposium, PL-TR-92-2210, ADA256711.
- Barker, T. G., K. L. McLaughlin and J. L. Stevens (1992), "Numerical Simulation of Quarry Blast Sources," S-CUBED Technical Report to DARPA, SSS-TR-93-13859.
- Gupta, I. N., K. L. McLaughlin, R. A. Wagner, T. W. McElfresh, and M. E. Marshall (1987), "Miscellaneous Studies in Decoupling," Teledyne Geotech Annual Report TGAL-87-4.
- Mueller, R. A. and J. R. Murphy (1971), "Seismic Characteristics of Underground Nuclear Detonations. Part I. Seismic Spectrum Scaling," *Bull. Seism. Soc. Am.*, 61, 1975.
- Murphy, J. R. (1969), "Discussion of Paper by Dr. Springer, M. Denny, J. Healy and W. Mickey, *The Sterling Experiment: Decoupling of Seismic Waves by a Shot-Generated Cavity*," *J. Geophys. Res.*, 74, p. 6714.
- Office of Technology Assessment (1988), "Seismic Verification of Nuclear Testing Treaties," OTA-SC-361, Government Printing Office, Washington, D.C.
- Perret, W. R. (1968a), "Free-Field Particle Motion from a Nuclear Explosion in Salt, Part I," Sandia Laboratory Report VUF-3012.
- Perret, W. R. (1986b), "Free-Field Ground Motion Study, Project Sterling," Sandia Laboratory Report SC-RR-68-410.
- Rimer, N., W. Proffer, E. Halda and R. Nilson (1993), "Containment Related Phenomenology From Chemical Kiloton," S-CUBED Technical Report to DNA, SSS-DTR-94-14405.
- Ringdal, F., G. B. Young and D. R. Baumgardt (1983), "Study of Detection and Location Techniques for Seismic Events Near Azgir, USSR: I. NORSAR Detection and Location Results," Technical Report No. 1, SAS-TR-82-01, ENSCO Inc.

- Rivière-Barbier, F. (1993), "Status Report on the Cooperative Research Program Between the EME and the CSS for Exchange and Analysis of Seismic Data from Quarry Blasts in Russia and in the U.S.." DARPA Center for Seismic Studies Report C93-01.**
- Springer, D., M. Denny, J. Healy and W. Mickey (1968), "The Sterling Experiment: Decoupling of Seismic Waves by a Shot-Generated Cavity," *J. Geophys. Res.*, 73, pp. 5995-6011.**
- Stevens, J. L., N. Rimer, J. R. Murphy, T. G. Barker, E. Bailey, E. J. Halda, W. J. Proffer, S. H. Rogers and B. Shkoller (1991), "Simulation of Seismic Signals from Partially Coupled Explosions in Spherical and Ellipsoidal Cavities," S-CUBED Final Report SSS-FR-91-12735.**

Prof. Thomas Ahrens
Seismological Lab, 252-21
Division of Geological & Planetary Sciences
California Institute of Technology
Pasadena, CA 91125

Prof. Keiiti Aki
Center for Earth Sciences
University of Southern California
University Park
Los Angeles, CA 90089-0741

Prof. Shelton Alexander
Geosciences Department
403 Deike Building
The Pennsylvania State University
University Park, PA 16802

Prof. Charles B. Archambeau
CIRES
University of Colorado
Boulder, CO 80309

Dr. Thomas C. Bache, Jr.
Science Applications Int'l Corp.
10260 Campus Point Drive
San Diego, CA 92121 (2 copies)

Prof. Muawia Barazangi
Institute for the Study of the Continent
Cornell University
Ithaca, NY 14853

Dr. Jeff Barker
Department of Geological Sciences
State University of New York
at Binghamton
Vestal, NY 13901

Dr. Douglas R. Baumgardt
ENSCO, Inc
5400 Port Royal Road
Springfield, VA 22151-2388

Dr. Susan Beck
Department of Geosciences
Building #77
University of Arizona
Tucson, AZ 85721

Dr. T.J. Bennett
S-CUBED
A Division of Maxwell Laboratories
11800 Sunrise Valley Drive, Suite 1212
Reston, VA 22091

Dr. Robert Blandford
AFTAC/TT, Center for Seismic Studies
1300 North 17th Street
Suite 1450
Arlington, VA 22209-2308

Dr. Stephen Bratt
ARPA/NMRO
3701 North Fairfax Drive
Arlington, VA 22203-1714

Dr. Lawrence Burdick
IGPP, A-025
Scripps Institute of Oceanography
University of California, San Diego
La Jolla, CA 92093

Dr. Robert Burrige
Schlumberger-Doll Research Center
Old Quarry Road
Ridgefield, CT 06877

Dr. Jerry Carter
Center for Seismic Studies
1300 North 17th Street
Suite 1450
Arlington, VA 22209-2308

Dr. Eric Chael
Division 9241
Sandia Laboratory
Albuquerque, NM 87185

Dr. Martin Chapman
Department of Geological Sciences
Virginia Polytechnical Institute
21044 Derring Hall
Blacksburg, VA 24061

Mr Robert Cockerham
Arms Control & Disarmament Agency
320 21st Street North West
Room 5741
Washington, DC 20451,

Prof. Vernon F. Cormier
Department of Geology & Geophysics
U-45, Room 207
University of Connecticut
Storrs, CT 06268

Prof. Steven Day
Department of Geological Sciences
San Diego State University
San Diego, CA 92182

Marvin Denny
U.S. Department of Energy
Office of Arms Control
Washington, DC 20585

Dr. Zoltan Der
ENSCO, Inc.
5400 Port Royal Road
Springfield, VA 22151-2388

Prof. Adam Dziewonski
Hoffman Laboratory, Harvard University
Dept. of Earth Atmos. & Planetary Sciences
20 Oxford Street
Cambridge, MA 02138

Prof. John Ebel
Department of Geology & Geophysics
Boston College
Chestnut Hill, MA 02167

Eric Fielding
SNEE Hall
INSTOC
Cornell University
Ithaca, NY 14853

Dr. Petr Firbas
Institute of Physics of the Earth
Masaryk University Brno
Jecna 29a
612 46 Brno, Czech Republic

Dr. Mark D. Fisk
Mission Research Corporation
735 State Street
P.O. Drawer 719
Santa Barbara, CA 93102

Prof Stanley Flatte
Applied Sciences Building
University of California, Santa Cruz
Santa Cruz, CA 95064

Prof. Donald Forsyth
Department of Geological Sciences
Brown University
Providence, RI 02912

Dr. Art Frankel
U.S. Geological Survey
922 National Center
Reston, VA 22092

Dr. Cliff Frolich
Institute of Geophysics
8701 North Mopac
Austin, TX 78759

Dr. Holly Given
IGPP, A-025
Scripps Institute of Oceanography
University of California, San Diego
La Jolla, CA 92093

Dr. Jeffrey W. Given
SAIC
10260 Campus Point Drive
San Diego, CA 92121

Dr. Dale Glover
Defense Intelligence Agency
ATTN: ODT-1B
Washington, DC 20301

Dan N. Hagedorn
Pacific Northwest Laboratories
Battelle Boulevard
Richland, WA 99352

Dr. James Hannon
Lawrence Livermore National Laboratory
P.O. Box 808
L-205
Livermore, CA 94550

Prof. David G. Harkrider
Seismological Laboratory
Division of Geological & Planetary Sciences
California Institute of Technology
Pasadena, CA 91125

Prof. Danny Harvey
CIRES
University of Colorado
Boulder, CO 80309

Prof. Donald V. Helmberger
Seismological Laboratory
Division of Geological & Planetary Sciences
California Institute of Technology
Pasadena, CA 91125

Prof. Eugene Herrin
Institute for the Study of Earth and Man
Geophysical Laboratory
Southern Methodist University
Dallas, TX 75275

Prof. Robert B. Herrmann
Department of Earth & Atmospheric Sciences
St. Louis University
St. Louis, MO 63156

Prof. Lane R. Johnson
Seismographic Station
University of California
Berkeley, CA 94720

Prof. Thomas H. Jordan
Department of Earth, Atmospheric &
Planetary Sciences
Massachusetts Institute of Technology
Cambridge, MA 02139

Prof. Alan Kafka
Department of Geology & Geophysics
Boston College
Chestnut Hill, MA 02167

Robert C. Kemerait
ENSCO, Inc.
445 Pineda Court
Melbourne, FL 32940

Dr. Karl Koch
Institute for the Study of Earth and Man
Geophysical Laboratory
Southern Methodist University
Dallas, Tx 75275

Dr. Max Koontz
U.S. Dept. of Energy/DP 5
Forrestal Building
1000 Independence Avenue
Washington, DC 20585

Dr. Richard LaCoss
MIT Lincoln Laboratory, M-200B
P.O. Box 73
Lexington, MA 02173-0073

Dr. Fred K. Lamb
University of Illinois at Urbana-Champaign
Department of Physics
1110 West Green Street
Urbana, IL 61801

Prof. Charles A. Langston
Geosciences Department
403 Deike Building
The Pennsylvania State University
University Park, PA 16802

Jim Lawson, Chief Geophysicist
Oklahoma Geological Survey
Oklahoma Geophysical Observatory
P.O. Box 8
Leonard, OK 74043-0008

Prof. Thorne Lay
Institute of Tectonics
Earth Science Board
University of California, Santa Cruz
Santa Cruz, CA 95064

Dr. William Leith
U.S. Geological Survey
Mail Stop 928
Reston, VA 22092

Mr. James F. Lewkowicz
Phillips Laboratory/GPEH
29 Randolph Road
Hanscom AFB, MA 01731-3010(2 copies)

Mr. Alfred Lieberman
ACDA/VI-OA State Department Building
Room 5726
320-21st Street, NW
Washington, DC 20451

Prof. L. Timothy Long
School of Geophysical Sciences
Georgia Institute of Technology
Atlanta, GA 30332

Dr. Randolph Martin, III
New England Research, Inc.
76 Olcott Drive
White River Junction, VT 05001

Dr. Robert Masse
Denver Federal Building
Box 25046, Mail Stop 967
Denver, CO 80225

Dr. Gary McCartor
Department of Physics
Southern Methodist University
Dallas, TX 75275

Prof. Thomas V. McEvilly
Seismographic Station
University of California
Berkeley, CA 94720

Dr. Art McGarr
U.S. Geological Survey
Mail Stop 977
U.S. Geological Survey
Menlo Park, CA 94025

Dr. Keith L. McLaughlin
S-CUBED
A Division of Maxwell Laboratory
P.O. Box 1620
La Jolla, CA 92038-1620

Stephen Miller & Dr. Alexander Florence
SRI International
333 Ravenswood Avenue
Box AF 116
Menlo Park, CA 94025-3493

Prof. Bernard Minster
IGPP, A-025
Scripps Institute of Oceanography
University of California, San Diego
La Jolla, CA 92093

Prof. Brian J. Mitchell
Department of Earth & Atmospheric Sciences
St. Louis University
St. Louis, MO 63156

Mr. Jack Murphy
S-CUBED
A Division of Maxwell Laboratory
11800 Sunrise Valley Drive, Suite 1212
Reston, VA 22091 (2 Copies)

Dr. Keith K. Nakanishi
Lawrence Livermore National Laboratory
L-025
P.O. Box 808
Livermore, CA 94550

Prof. John A. Orcutt
IGPP, A-025
Scripps Institute of Oceanography
University of California, San Diego
La Jolla, CA 92093

Prof. Jeffrey Park
Kline Geology Laboratory
P.O. Box 6666
New Haven, CT 06511-8130

Dr. Howard Patton
Lawrence Livermore National Laboratory
L-025
P.O. Box 808
Livermore, CA 94550

Dr. Frank Pilotte
HQ AFTAC/TT
1030 South Highway A1A
Patrick AFB, FL 32925-3002

Dr. Jay J. Pulli
Radix Systems, Inc.
201 Perry Parkway
Gaithersburg, MD 20877

Dr. Robert Reinke
ATTN: FCTVTD
Field Command
Defense Nuclear Agency
Kirtland AFB, NM 87115

Prof. Paul G. Richards
Lamont-Doherty Geological Observatory
of Columbia University
Palisades, NY 10964

Mr. Wilmer Rivers
Teledyne Geotech
314 Montgomery Street
Alexandria, VA 22314

Dr. Alan S. Ryall, Jr.
ARPA/NMRO
3701 North Fairfax Drive
Arlington, VA 22203-1714

Dr. Richard Sailor
TASC, Inc.
55 Walkers Brook Drive
Reading, MA 01867

Prof. Charles G. Sammis
Center for Earth Sciences
University of Southern California
University Park
Los Angeles, CA 90089-0741

Prof. Christopher H. Scholz
Lamont-Doherty Geological Observatory
of Columbia University
Palisades, NY 10964

Dr. Susan Schwartz
Institute of Tectonics
1156 High Street
Santa Cruz, CA 95064

Secretary of the Air Force
(SAFRD)
Washington, DC 20330

Brian Stump
Los Alamos National Laboratory
EES-3, Mail Stop C335
Los Alamos, NM 87545

Office of the Secretary of Defense
DDR&E
Washington, DC 20330

Prof. Jeremiah Sullivan
University of Illinois at Urbana-Champaign
Department of Physics
1110 West Green Street
Urbana, IL 61801

Thomas J. Sereno, Jr.
Science Application Int'l Corp.
10260 Campus Point Drive
San Diego, CA 92121

Prof. L. Sykes
Lamont-Doherty Geological Observatory
of Columbia University
Palisades, NY 10964

Dr. Michael Shore
Defense Nuclear Agency/SPSS
6801 Telegraph Road
Alexandria, VA 22310

Dr. David Taylor
ENSCO, Inc.
445 Pineda Court
Melbourne, FL 32940

Dr. Robert Shumway
University of California Davis
Division of Statistics
Davis, CA 95616

Dr. Steven R. Taylor
Los Alamos National Laboratory
P.O. Box 1663
Mail Stop C335
Los Alamos, NM 87545

Dr. Matthew Sibol
Virginia Tech
Seismological Observatory
4044 Derring Hall
Blacksburg, VA 24061-0420

Prof. Clifford Thurber
University of Wisconsin-Madison
Department of Geology & Geophysics
1215 West Dayton Street
Madison, WI 53706

Prof. David G. Simpson
IRIS, Inc.
1616 North Fort Myer Drive
Suite 1050
Arlington, VA 22209

Prof. M. Nafi Toksoz
Earth Resources Lab
Massachusetts Institute of Technology
42 Carleton Street
Cambridge, MA 02142

Donald L. Springer
Lawrence Livermore National Laboratory
L-025
P.O. Box 808
Livermore, CA 94550

Dr. Larry Turnbull
CIA-OSWR/NED
Washington, DC 20505

Dr. Jeffrey Stevens
S-CUBED
A Division of Maxwell Laboratory
P.O. Box 1620
La Jolla, CA 92038-1620

Dr. Gregory van der Vink
IRIS, Inc.
1616 North Fort Myer Drive
Suite 1050
Arlington, VA 22209

Lt. Col. Jim Stobie
ATTN: AFOSR/NL
110 Duncan Avenue
Bolling AFB
Washington, DC 20332-0001

Dr. Karl Veith
EG&G
5211 Auth Road
Suite 240
Suitland, MD 20746

Prof. Terry C. Wallace
Department of Geosciences
Building #77
University of Arizona
Tucson, AZ 85721

Phillips Laboratory
ATTN: XPG
29 Randolph Road
Hanscom AFB, MA 01731-3010

Dr. Thomas Weaver
Los Alamos National Laboratory
P.O. Box 1663
Mail Stop C335
Los Alamos, NM 87545

Phillips Laboratory
ATTN: GPE
29 Randolph Road
Hanscom AFB, MA 01731-3010

Dr. William Wortman
Mission Research Corporation
8560 Cinderbed Road
Suite 700
Newington, VA 22122

Phillips Laboratory
ATTN: TSML
5 Wright Street
Hanscom AFB, MA 01731-3004

Prof. Francis T. Wu
Department of Geological Sciences
State University of New York
at Binghamton
Vestal, NY 13901

Phillips Laboratory
ATTN: PL/SUL
3550 Aberdeen Ave SE
Kirtland, NM 87117-5776 (2 copies)

Prof Ru-Shan Wu
University of California, Santa Cruz
Earth Sciences Department
Santa Cruz
, CA 95064

Dr. Michel Bouchon
I.R.I.G.M.-B.P. 68
38402 St. Martin D'Heres
Cedex, FRANCE

ARPA, OASB/Library
3701 North Fairfax Drive
Arlington, VA 22203-1714

Dr. Michel Campillo
Observatoire de Grenoble
I.R.I.G.M.-B.P. 53
38041 Grenoble, FRANCE

HQ DNA
ATTN: Technical Library
Washington, DC 20305

Dr. Kin Yip Chun
Geophysics Division
Physics Department
University of Toronto
Ontario, CANADA

Defense Intelligence Agency
Directorate for Scientific & Technical Intelligence
ATTN: DTIB
Washington, DC 20340-6158

Prof. Hans-Peter Harjes
Institute for Geophysics
Ruhr University/Bochum
P.O. Box 102148
4630 Bochum 1, GERMANY

Defense Technical Information Center
Cameron Station
Alexandria, VA 22314 (2 Copies)

Prof. Eystein Husebye
NTNF/NORSAR
P.O. Box 51
N-2007 Kjeller, NORWAY

TACTEC
Battelle Memorial Institute
505 King Avenue
Columbus, OH 43201 (Final Report)

David Jepsen
Acting Head, Nuclear Monitoring Section
Bureau of Mineral Resources
Geology and Geophysics
G.P.O. Box 378, Canberra, AUSTRALIA

Ms. Eva Johannisson
Senior Research Officer
FOA
S-172 90 Sundbyberg, SWEDEN

Dr. Peter Marshall
Procurement Executive
Ministry of Defense
Blacknest, Brimpton
Reading FG7-FRS, UNITED KINGDOM

Dr. Bernard Massinon, Dr. Pierre Mechler
Societe Radiomana
27 rue Claude Bernard
75005 Paris, FRANCE (2 Copies)

Dr. Svein Mykkeltveit
NTNT/NORSAR
P.O. Box 51
N-2007 Kjeller, NORWAY (3 Copies)

Prof. Keith Priestley
University of Cambridge
Bullard Labs, Dept. of Earth Sciences
Madingley Rise, Madingley Road
Cambridge CB3 0EZ, ENGLAND

Dr. Jorg Schlittenhardt
Federal Institute for Geosciences & Nat'l Res.
Postfach 510153
D-30631 Hannover, GERMANY

Dr. Johannes Schweitzer
Institute of Geophysics
Ruhr University/Bochum
P.O. Box 1102148
4360 Bochum 1, GERMANY

Trust & Verify
VERTIC
Carrara House
20 Embankment Place
London WC2N 6NN, ENGLAND